[redacted]

[redacted]

NASA TECHNICAL MEMORANDUM

NASA TM X-3211

NASA TM X-3211

CONFIDENTIAL	CLASSIFIED
BY Security Classification Officer, NASA LaRC	
SUBJECT TO GENERAL DECLASSIFICATION SCHEDULE OF EXECUTIVE ORDER 11652 AUTOMATICALLY DOWNGRADED AT TWO YEAR INTERVALS AND DECLASSIFIED ON DEC 31 1981	

STATIC LONGITUDINAL AERODYNAMIC CHARACTERISTICS OF A MODEL WITH A MODIFIED 17-PERCENT-THICK SUPERCRITICAL WING (U)

James C. Ferris

Langley Research Center
Hampton, Va. 23665

NATIONAL AERONAUTICS AND SPACE ADMINISTRATION • WASHINGTON, D. C. • MAY 1975

[redacted]

[redacted]

1 Report No	2 Government Accession No	3 Recipient's Catalog No
NASA TM X-3211		

4 Title and Subtitle	5 Report Date
STATIC LONGITUDINAL AERODYNAMIC CHARACTERISTICS OF A MODEL WITH A MODIFIED 17-PERCENT-THICK SUPERCRITICAL WING (U)	May 1975
	6 Performing Organization Code
7 Author(s)	8 Performing Organization Report No
James C. Ferris	L-9960
	10 Work Unit No
9 Performing Organization Name and Address	505-11-11-04
NASA Langley Research Center Hampton, Va. 23665	11 Contract or Grant No
	13 Type of Report and Period Covered
12 Sponsoring Agency Name and Address	Technical Memorandum
National Aeronautics and Space Administration Washington, D.C. 20546	14 Sponsoring Agency Code

15 Supplementary Notes

16 Abstract

An investigation was made of the static longitudinal stability characteristics of a 0.09-scale model of an airplane with a modified 17-percent-thick supercritical wing. Modifications were made to the wing to reduce a gradual buildup of boundary-layer shock loss preceding drag divergence (drag creep) noted in an earlier investigation. The longitudinal aerodynamic characteristics were determined over a Mach number range from 0.30 to 0.76 at angles of attack that generally provided a lift-coefficient range from 0 to buffet onset.

17 Key Words (Suggested by Author(s))	18 Distribution Statement
Supercritical airfoil Thick wing	Confidential – Available to U.S. Government Agencies and Their Contractors Only New Subject Category 02

19 Security Classif. (of this report)	20 Security Classif (of this page)	21 No of Pages	22 Price
[redacted]	Unclassified	37	

[redacted] NAL SECURITY [redacted] ON"
Unauth[redacted] minal Sanctions

CONFIDENTIAL CLASSIFIED
BY Security Classification Officer, NASA LaRC
SUBJECT TO GENERAL DECLASSIFICATION SCHEDULE OF EXECUTIVE ORDER 11652 AUTOMATICALLY DOWNGRADED AT TWO YEAR INTERVALS AND DECLASSIFIED ON DEC 31
1981

[redacted]

[redacted]

STATIC LONGITUDINAL AERODYNAMIC CHARACTERISTICS OF A MODEL WITH A MODIFIED 17-PERCENT-THICK SUPERCRITICAL WING (U)

James C. Ferris
Langley Research Center

SUMMARY

An investigation was made of the static longitudinal stability characteristics of a 0.09-scale model of an airplane with a modified 17-percent-thick supercritical wing. Modifications were made to the wing to reduce a gradual buildup of boundary-layer shock loss preceding drag divergence (drag creep) noted in an earlier investigation. The longitudinal aerodynamic characteristics were determined over a Mach number range from 0.30 to 0.76 at angles of attack that generally provided a lift-coefficient range from 0 to buffet onset.

Results of the investigation indicate that the modifications to the airfoil essentially eliminated the drag creep associated with the airfoil that occurs between the critical Mach number (the free-stream Mach number at which the local velocity becomes sonic at some point on the airfoil) and the drag-divergence Mach number M_{DD}. These modifications also reduced the minimum drag at all test Mach numbers and the drag due to lift at Mach numbers of 0.70 and 0.73.

INTRODUCTION

The advantages of the supercritical airfoil have been realized on a wide range of aerodynamic configurations. Supercritical airfoils have been applied to transport aircraft to increase cruise speeds, to variable-wing-sweep fighter airplanes to improve transonic maneuvering performance (ref. 1), and to propellers to allow higher propeller tip speeds. In all cases, application of the supercritical airfoil has enhanced the performance of the configuration and in many cases, improved other characteristics of the design. For example, the excellent low-speed characteristics of the research airplane with a supercritical wing for which data are presented in references 2 to 6 generated considerable new interest in high-thickness-ratio airfoils, especially in the general aviation (see ref. 7) and STOL transport areas.

[redacted]

One problem with the research airplane of reference 2 was a gradual buildup of boundary-layer shock loss preceding drag divergence (drag creep) at the higher Mach numbers. Although analysis of these previous results indicated that part of the drag creep was due to adverse wing-fuselage interference, wing section drag measurements indicated that part of the creep was due to the airfoil itself. Recent two-dimensional airfoil research on a 10-percent-thick airfoil has been directed toward reducing this drag creep, and data from this wind-tunnel investigation are presented in reference 8. Comparison of an experimentally designed supercritical airfoil with a theoretically designed one is presented in reference 9.

The purpose of the present report is to present longitudinal aerodynamic results from a wind-tunnel investigation that used a modified 17-percent-thick airfoil (based on the two-dimensional studies of ref. 8). The results of this investigation showed improvement in the drag creep characteristics of the original research airplane model with a thick supercritical wing. (See ref. 2.)

The investigation was conducted in the Langley 8-foot transonic pressure tunnel. Data were obtained at Mach numbers from 0.30 to 0.76 for the basic configuration (configuration 2). Modifications to the airfoil were made, and data were obtained at Mach numbers from 0.50 to 0.75 for the modified configurations (configurations 4 and 8).

SYMBOLS

The longitudinal results are referred to the stability-axis system. The origin of the stability axes is at the moment reference center, located at 25 percent of the reference length ($\bar{c}$) and 1.084 cm above the fuselage reference line. (See fig. 1.) All data presented herein are based on the planform dimensions of the wing.

b	reference span, 98.618 centimeters
c	local chord, centimeters
$\bar{c}$	model reference length, 20.318 centimeters
C_D	drag coefficient, $\frac{\text{Drag}}{qS}$
C_L	lift coefficient, $\frac{\text{Lift}}{qS}$
C_{L_α}	lift-curve slope, $\frac{\partial C_L}{\partial \alpha}$, per degree

[redacted]

C_m pitching-moment coefficient, $\frac{\text{Pitching moment}}{qS\bar{c}}$

$C_{m_{C_L}}$ longitudinal stability derivative, $\frac{\partial C_m}{\partial C_L}$

$C_{m,o}$ pitching-moment coefficient at zero lift

L/D lift-drag ratio

M free-stream Mach number

M_{DD} drag-divergence Mach number, Mach number for which $\frac{\partial C_D}{\partial M} = 0.1$

p_t free-stream total pressure, newtons per square meter

q free-stream dynamic pressure, newtons per square meter

R Reynolds number based on model reference length

S reference wing area, 0.192 square meter

x ordinate along airfoil reference line measured from airfoil leading edge, centimeters

y spanwise distance from plane of symmetry, centimeters

z ordinate normal to airfoil reference line, centimeters

α angle of attack referred to fuselage reference line, degrees

Subscript:

max maximum

APPARATUS AND PROCEDURES

Model Description

The model of the present investigation was a sting-supported 0.09-scale model of an airplane with an unswept wing employing supercritical airfoil sections having a constant

[redacted]

spanwise thickness ratio of 17 percent. Figures 1 and 2 are drawings and photographs of the model; the geometric characteristics are presented in table I. Table II contains coordinates of the airfoil for the original model (configuration 2 of this investigation) at a semispan station of 0.4245, and table III contains coordinates for the final configuration (configuration 8) at semispan stations of 0.4245 and 0.7325. Airfoil sketches are shown in figures 1(b) and 1(c). Of the configurations investigated, data are presented for configurations 2, 4, and 8 only, since the other minor changes had no significant effect on the aerodynamic characteristics. Configuration 4 was a modification of the forward half of the airfoil only; it had the coordinates of configuration 8 over the forward 50 percent of the airfoil and those of configuration 2 over the aft 50 percent of the airfoil.

The incidence of the horizontal tail and the deflection of the elevator were maintained at 0° for this investigation.

Tunnel Description

The investigation was conducted in the Langley 8-foot transonic pressure tunnel, which is a single-return tunnel having a rectangular slotted test section to permit continuous operation through the transonic speed range. This facility has the capability of independent variation of Mach number, density, temperature, and humidity. The stagnation temperature and dewpoint were maintained at values sufficient to avoid significant condensation effects.

Measurements

Six-component force and moment data were obtained with an electrical strain-gage balance housed within the fuselage. Measurements were made at Mach numbers from 0.30 to 0.76 and over an angle-of-attack range that generally provided a lift-coefficient range from 0 to buffet onset (approximately -4° to 6°). The wind-tunnel conditions for which the measurements were obtained are presented in table IV.

Boundary-Layer Transition

All tests were made with transition fixed on the model. Boundary-layer trips were applied to the upper and lower surfaces of the wing by use of the technique described in references 10 and 11 to simulate the displacement thickness of the turbulent boundary layer at the wing trailing edge for a full-scale Reynolds number. This technique requires that laminar flow be maintained ahead of the trips, and as a result, model surface regions ahead of the trips were maintained in an extremely smooth condition.

The location and the size of the grains used for the boundary-layer trips are shown in the following table:

Surface	Type of transition strip	Location
Fuselage	No. 150 carborundum grains	3.1 cm aft of nose apex
Wing upper surface	No. 120 carborundum grains	27 percent of local streamwise chord
Wing lower surface	No. 120 carborundum grains	37 percent of local streamwise chord
Wing-tip-mounted fuel tanks	No. 150 carborundum grains	3.3 cm aft of nose apex
Horizontal and vertical tails	No. 180 carborundum grains	10 percent of local streamwise chord

Corrections

The drag data have been adjusted to the condition of free-stream static pressure acting over the fuselage cavity and base areas. Corrections have been made to the angle of attack for model support sting and balance deflections, which occur as a result of aerodynamic loads on the model. Further corrections to the measured angle of attack have been made for tunnel airflow angularity and for the first-order boundary correction calculated by the methods of reference 12.

Accuracy

The accuracies of the individual measured quantities, based on calibrations and repeatability of the data, are estimated to be within the following limits:

C_L	±0.008
C_D	±0.0007
C_m	±0.0020
α, deg	±0.07
M	±0.002
q, N/m^2	±70.0

DISCUSSION OF RESULTS

The basic longitudinal aerodynamic characteristics are presented in figure 3 and are summarized in figures 4 to 7. Results for configuration 4 are not included in the

summary data, since the values were not significantly different from those of configuration 8. The basic configuration (configuration 2) was investigated throughout the Mach number range (from 0.30 to 0.76) before modifications were made to the airfoil, since the fuselage had been modified to receive a sting support system through the top and a rudder was added to the vertical tail for spin studies. The configuration, therefore, differed slightly from that reported in reference 2.

Drag Characteristics

The results of figure 3 indicate that the minimum drag coefficient was reduced for the modified configurations throughout the Mach number range and that the reduction was greater at high Mach numbers. The drag due to lift was also reduced at Mach numbers of 0.70 and 0.73. The variation of drag as a function of Mach number is presented in figure 4. The drag creep associated with the airfoil occurs between the critical Mach number (the free-stream Mach number at which the local velocity becomes sonic at some point on the airfoil) and the drag-divergence Mach number. Comparison of the results of figure 4 with the section drag results of reference 3 for the unmodified airfoil suggests that the drag creep associated with the airfoil has been essentially eliminated. For example, at a lift coefficient of 0.4 between Mach numbers of 0.50 and 0.73, the difference between the total drag creep for configuration 2 and that for configuration 8 (presented in fig. 4) is about 0.0021. This value is about equal to the profile drag creep of the wing shown for the unmodified airfoil in figure 8 of reference 3. This improvement in drag for configuration 8 is a direct result of changes to the forward part of the airfoil and the associated reduction in induced velocities. The drag-divergence Mach number M_{DD} was not significantly changed by these modifications. The variation of untrimmed (the trim requirements for both configurations are about the same) maximum lift-drag ratio $(L/D)_{max}$ and lift coefficient at $(L/D)_{max}$ are presented in figure 5. Note that $(L/D)_{max}$ is improved for configuration 8 throughout the Mach number range and has increased by 10 percent at a cruise Mach number of 0.73. The lift coefficient at $(L/D)_{max}$ is also increased throughout the Mach number range.

Lift and Longitudinal Stability

The basic longitudinal stability data of figure 3 indicate some small changes for the modified wing. The stable break in the pitching-moment curves (abrupt increase in stability level) at Mach numbers of 0.70 and 0.73 is extended to higher lift coefficients for configurations 4 and 8. Increases in the lift coefficient for the modified configurations are observed throughout the Mach number and angle-of-attack ranges. As expected, the break in the lift curve is extended to higher lift coefficients at Mach numbers of 0.70 and 0.73. The data of figure 6 show a small increase in $C_{m,o}$ and in stability (decrease

[redacted]

in $C_{m_{C_L}}$) at high Mach numbers. The lift-curve slope C_{L_α} as a function of Mach number is shown in figure 7 for configuration 2 only, since C_{L_α} was not significantly changed for configurations 4 and 8. The increase in C_{L_α} at Mach numbers from 0.60 to 0.75 is a result of the development of a region of supersonic flow over the upper surface of the wing.

SUMMARY OF RESULTS

An investigation conducted in the Langley 8-foot transonic pressure tunnel at Mach numbers from 0.30 to 0.76 to determine the effects of airfoil modifications on drag creep for a thick unswept supercritical wing has indicated the following:

1. On the basis of comparisons with previous results, modifications to an original 17-percent-thick supercritical airfoil essentially eliminated that part of the drag creep associated with the airfoil, although the total aircraft combination does exhibit some drag creep.

2. These modifications also reduced the drag due to lift at a Mach number of 0.73 and resulted in a 10-percent increase in maximum untrimmed lift-drag ratio at this cruise Mach number.

3. Only slight changes were noted in the longitudinal stability and lift characteristics, and the stable break in the lift curve was extended to higher lift coefficients at Mach numbers of 0.70 and 0.73.

Langley Research Center,
National Aeronautics and Space Administration,
Hampton, Va., February 18, 1975.

[redacted]

[redacted]

REFERENCES

1. Hallissy, James B.: Longitudinal Aerodynamic Characteristics of a Carrier-Based Variable-Wing-Sweep Fighter Airplane With Partial Incorporation of the NASA Supercritical Airfoil. NASA TM X-2745, 1973.

2. Ferris, James C.: Static Aerodynamic Characteristics of a Model With a 17-Percent-Thick Supercritical Wing. NASA TM X-2551, 1972.

3. Ferris, James C.: Wind-Tunnel Measurements of the Chordwise Pressure Distribution and Profile Drag of a Research Airplane Model Incorporating a 17-Percent-Thick Supercritical Wing. NASA TM X-2760, 1973.

4. Palmer, W. E.; Elliott, D. W.; and White, J. E.: Flight and Wind Tunnel Evaluation of a 17% Thick Supercritical Airfoil on a T-2C Airplane. NR71H-150 (Contract N00019-70-C-0474), North Americal Rockwell Corp., July 31, 1971.
   Vol. I – Basic Report. (Available from DDC as AD 517 436L.)
   Vol. II – Flight Measured Wing Wake Profiles and Surface Pressures. (Available from DDC as AD 517 437L.)

5. Elliott, D. W.: Flying Qualities Evaluations of a 17% Thick Supercritical Wing on a T-2C Airplane. NR71H-331 (Contract N00019-70-C-0474, P00001), North American Rockwell Corp., July 1971. (Available from DDC as AD 518 964L.)

6. Elliott, D. W.; Palmer, W. E.; and White, J. E.: Evaluation of Boundary Layer Characteristics on a 17% Thick Supercritical Wing on a T-2C Airplane. NR72H-81 (Contract N00019-70-C-0474, P00002), North American Rockwell Corp., Mar. 1972. (Available from DDC as AD 521 336L.)

7. McGhee, Robert J.; and Beasley, William D.: Low-Speed Aerodynamic Characteristics of a 17-Percent-Thick Airfoil Section Designed for General Aviation Applications. NASA TN D-7428, 1973.

8. Harris, Charles D.: Aerodynamic Characteristics of an Improved 10-Percent-Thick NASA Supercritical Airfoil. NASA TM X-2978, 1974.

9. Harris, Charles D.: Comparison of the Experimental Aerodynamic Characteristics of Theoretically and Experimentally Designed Supercritical Airfoils. NASA TM X-3082, 1974.

10. Loving, Donald L.: Wind-Tunnel—Flight Correlation of Shock-Induced Separated Flow. NASA TN D-3580, 1966.

[redacted]

11. Blackwell, James A., Jr.: Preliminary Study of Effects of Reynolds Number and Boundary-Layer Transition Location on Shock-Induced Separation. NASA TN D-5003, 1969.

12. Wright, Ray H.; and Barger, Raymond L.: Wind-Tunnel Lift Interference on Swept-back Wings in Rectangular Test Sections With Slotted Top and Bottom Walls. NASA TR R-241, 1966.

[redacted]

TABLE I.- MODEL GEOMETRIC CHARACTERISTICS

Wing:	
Total area, m^2	0.192
Aileron area (one aileron), m^2	0.007
Span (theoretical), cm	98.618
Aspect ratio	5.07
Taper ratio	0.496
Dihedral angle, deg	3.323
Incidence at root, deg	2.5
Incidence at tip, deg	1
Airfoil at root and tip	See tables II and III
Mean aerodynamic chord, cm	20.318
Horizontal distance to center line of airplane, cm	21.735
Vertical distance to fuselage reference line at 25-percent-chord line, cm	1.084
Incidence, deg	2
Horizontal tail:	
Total area, m^2	0.054
Elevator area (total aft of hinge line), m^2	0.016
Span, cm	49.131
Aspect ratio	4.47
Taper ratio	0.508
Dihedral angle, deg	0
Airfoil at root and tip	NACA 65_1A012
Mean aerodynamic chord, cm	11.533
Horizontal distance to center of airplane, cm	10.923
Vertical distance to fuselage reference line at 25-percent-chord line, cm	13.076
Vertical tail:	
Total area (exposed), m^2	0.027
Rudder area, m^2	0.007
Span (theoretical, exposed), cm	22.055
Aspect ratio (exposed)	1.800
Taper ratio (exposed)	0.375
Airfoil at root and tip, cm	NACA 63_1A012
Mean aerodynamic chord, cm	13.385
Vertical distance to fuselage reference line, cm	16.848

[redacted]

[redacted]

TABLE II.- WING AIRFOIL COORDINATES ALONG STREAMWISE CHORDS AT SEMISPAN STATION $\frac{y}{b/2} = 0.4245$ FOR CONFIGURATION 2

$$\left[\frac{\text{Leading-edge radius}}{\text{Local chord}} = 0.0428\right]$$

x/c	z/c	
	Upper	Lower
0.0125	0.0292	-0.0312
.0250	.0397	-.0414
.0375	.0464	-.0482
.0500	.0518	-.0534
.0750	.0591	-.0606
.1000	.0648	-.0658
.1250	.0694	-.0700
.1500	.0733	-.0730
.1750	.0766	-.0756
.2000	.0792	-.0777
.2500	.0831	-.0804
.3000	.0861	-.0818
.3500	.0880	-.0816
.4000	.0892	-.0805
.4500	.0894	-.0780
.5000	.0885	-.0737
.5500	.0865	-.0675
.5750	.0852	-.0634
.6000	.0834	-.0587
.6250	.0815	-.0533
.6500	.0791	-.0477
.6750	.0765	-.0419
.7000	.0736	-.0359
.7250	.0696	-.0299
.7500	.0654	-.0239
.7750	.0612	-.0183
.8000	.0561	-.0131
.8250	.0504	-.0087
.8500	.0443	-.0052
.8750	.0376	-.0030
.9000	.0314	-.0013
.9250	.0237	-.0012
.9500	.0162	-.0022
.9750	.0090	-.0045
1.0000	0	-.0077

[redacted]

[redacted]

TABLE III.- WING AIRFOIL COORDINATES ALONG STREAMWISE CHORDS FOR CONFIGURATION 8

$$\left[\frac{\text{Leading-edge radius}}{\text{Local chord}} = 0.0428\right]$$

x/c	z/c at –			
	Semispan station $\frac{y}{b/2} = 0.4245$		Semispan station $\frac{y}{b/2} = 0.7325$	
	Lower	Upper	Lower	Upper
0.01	0.0262	-0.0268	0.0274	-0.0280
.02	.0354	-.0357	.0357	-.0366
.03	.0409	-.0422	.0411	-.0420
.04	.0454	-.0469	.0455	-.0466
.05	.0491	-.0506	0495	-.0504
.06	.0523	-.0540	0575	-.0536
.08	.0579	-.0591	.0578	-.0588
.10	.0627	-.0635	.0625	-.0628
.12	.0664	-.0671	.0662	-.0661
.14	.0690	- 0700	.0691	-.0692
.16	.0774	-.0724	.0718	-.0716
.18	.0749	-.0746	.0744	-.0742
.20	.0770	-.0763	.0764	-.0759
.25	.0816	-.0793	.0810	-.0789
.30	.0850	-.0805	.0845	-.0809
.35	.0875	-.0805	.0869	-.0817
.40	.0890	-.0793	.0880	-.0806
.45	.0889	-.0770	0880	-.0778
.50	.0878	-.0724	.0870	-.0735
.55	.0858	-.0666	.0850	-.0675
.60	.0825	-.0582	.0818	-.0589
.62	.0807	-.0543	.0802	-.0550
.64	.0789	-.0492	.0783	-.0506
.66	.0769	-.0442	.0763	-.0460
.68	.0744	-.0391	.0738	-.0409
.70	.0716	-.0346	.0712	-.0360
.72	.0684	-.0292	.0683	-.0311
.74	.0652	-.0243	.0646	-.0265
.76	.0617	-.0197	.0610	-.0222
.78	.0574	-.0154	.0571	-.0180
.80	.0532	-.0114	.0531	-.0141
.82	.0490	-.0078	.0486	-.0107
.84	.0441	-.0050	.0437	-.0078
.86	.0392	-.0026	.0388	-.0055
.88	.0344	-.0008	.0341	-.0036
.90	.0290	+.0008	.0289	-.0024
.92	.0240	+.0012	.0234	-.0022
.94	.0185	+.0006	.0180	-.0026
.96	.0129	-.0008	.0125	-.0040
.98	.0069	-.0033	.0066	-.0065
1.00	0	-.0070	0	-.0095

[redacted]

TABLE IV.- WIND-TUNNEL OPERATING CONDITIONS

Mach number	p_t, N/m^2	q, N/m^2	R
0.30	170 837	10 112	2.00×10^6
.50	146 561	21 618	2.66
.60	159 872	31 591	3.33
.65	175 720	39 133	3.86
.70	167 677	41 466	3.86
.73	163 655	42 828	3.86
.75	161 165	43 692	3.86
.76	160 016	44 132	3.86

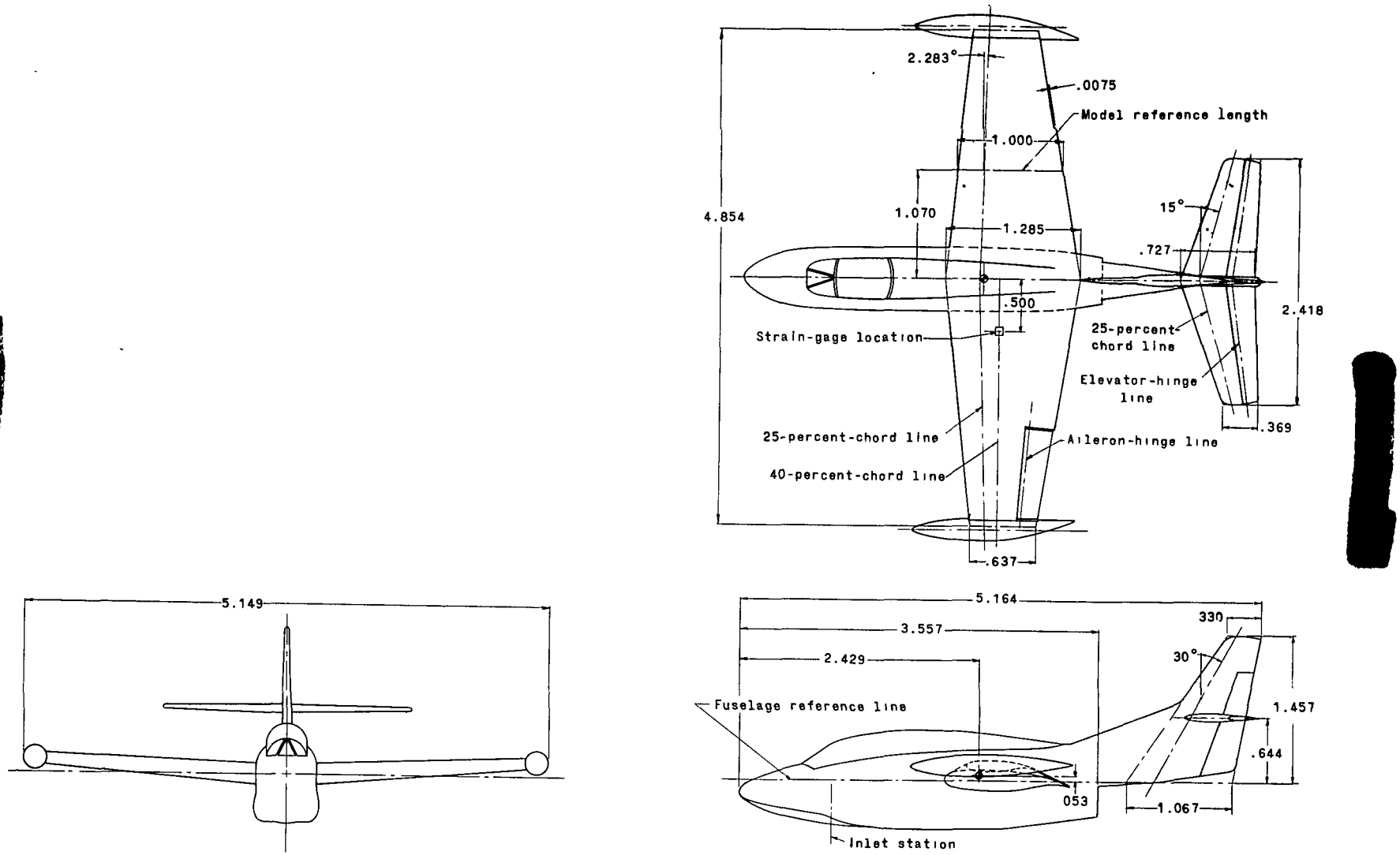

(a) General arrangement of model.

Figure 1.- Drawings of the wind-tunnel model. All dimensions are in terms of model reference length, 20.318 cm.

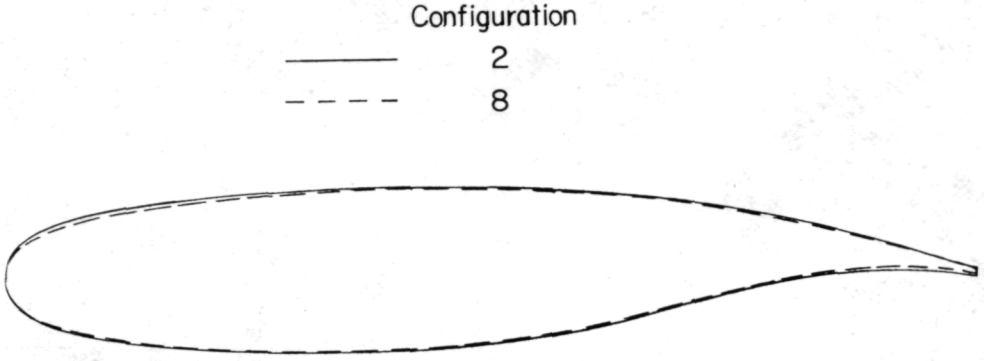

(b) Airfoil sketches.

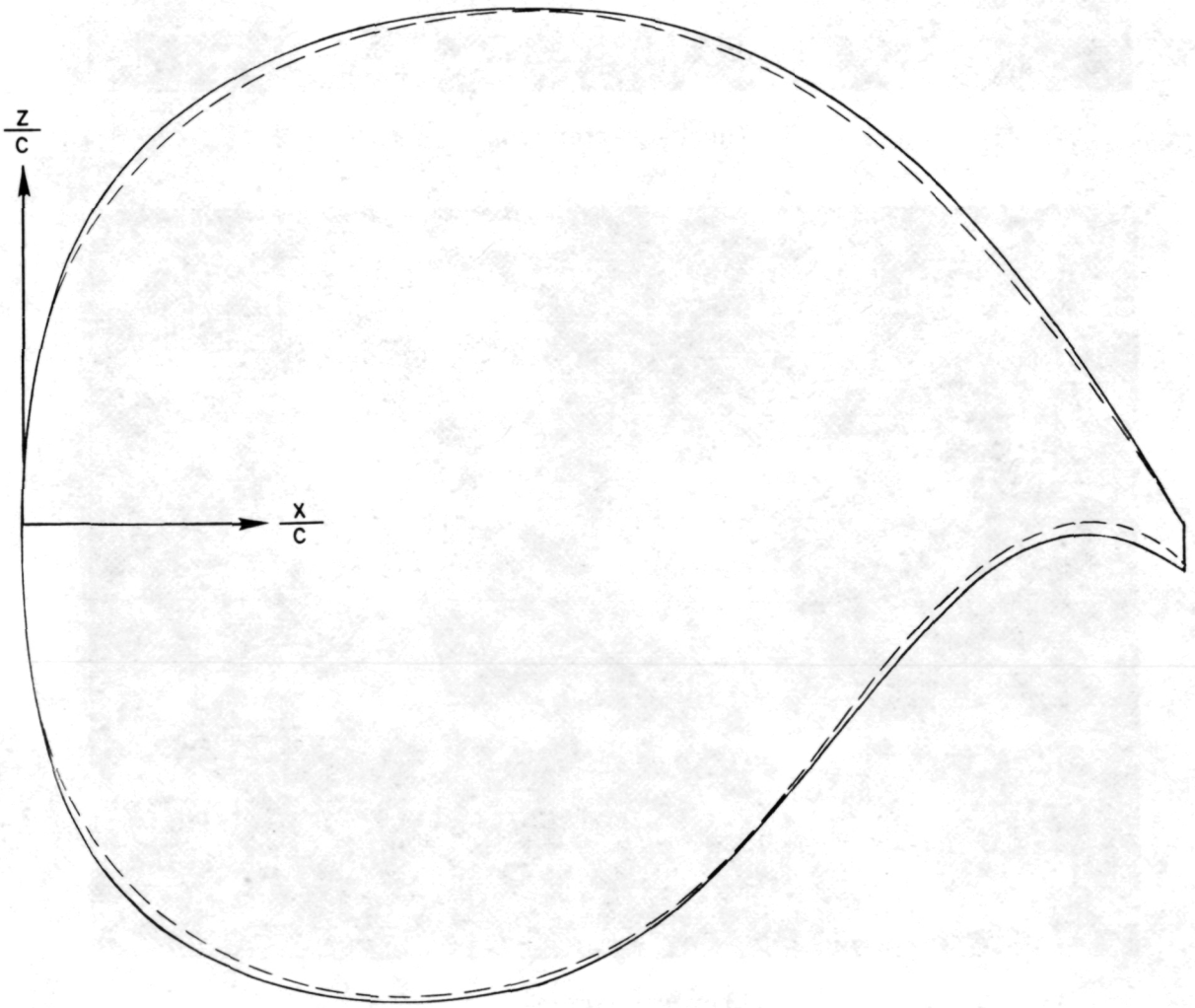

(c) Airfoil sketches with z/c-scale expanded.

Figure 1.- Concluded.

Page Intentionally Left Blank

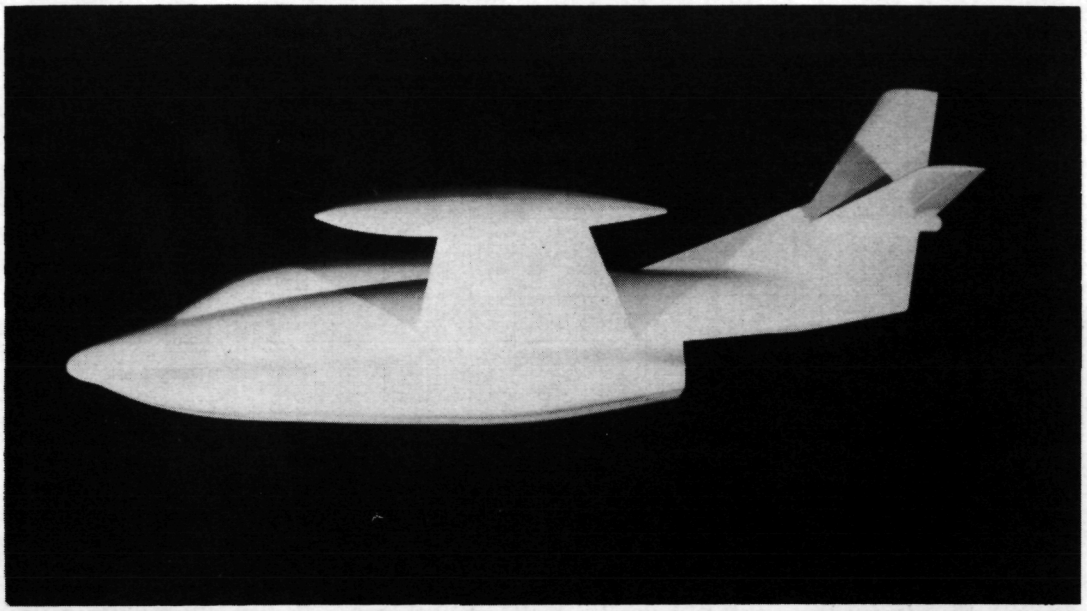

L-70-6041

Lower side view

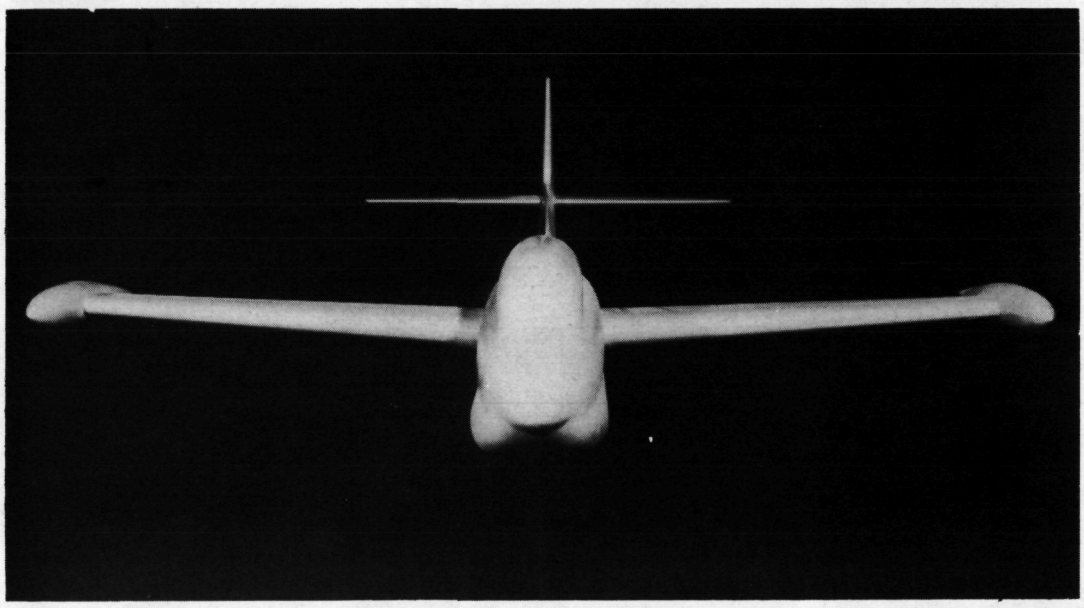

L-70-6040

Front view

Figure 2.- Concluded.

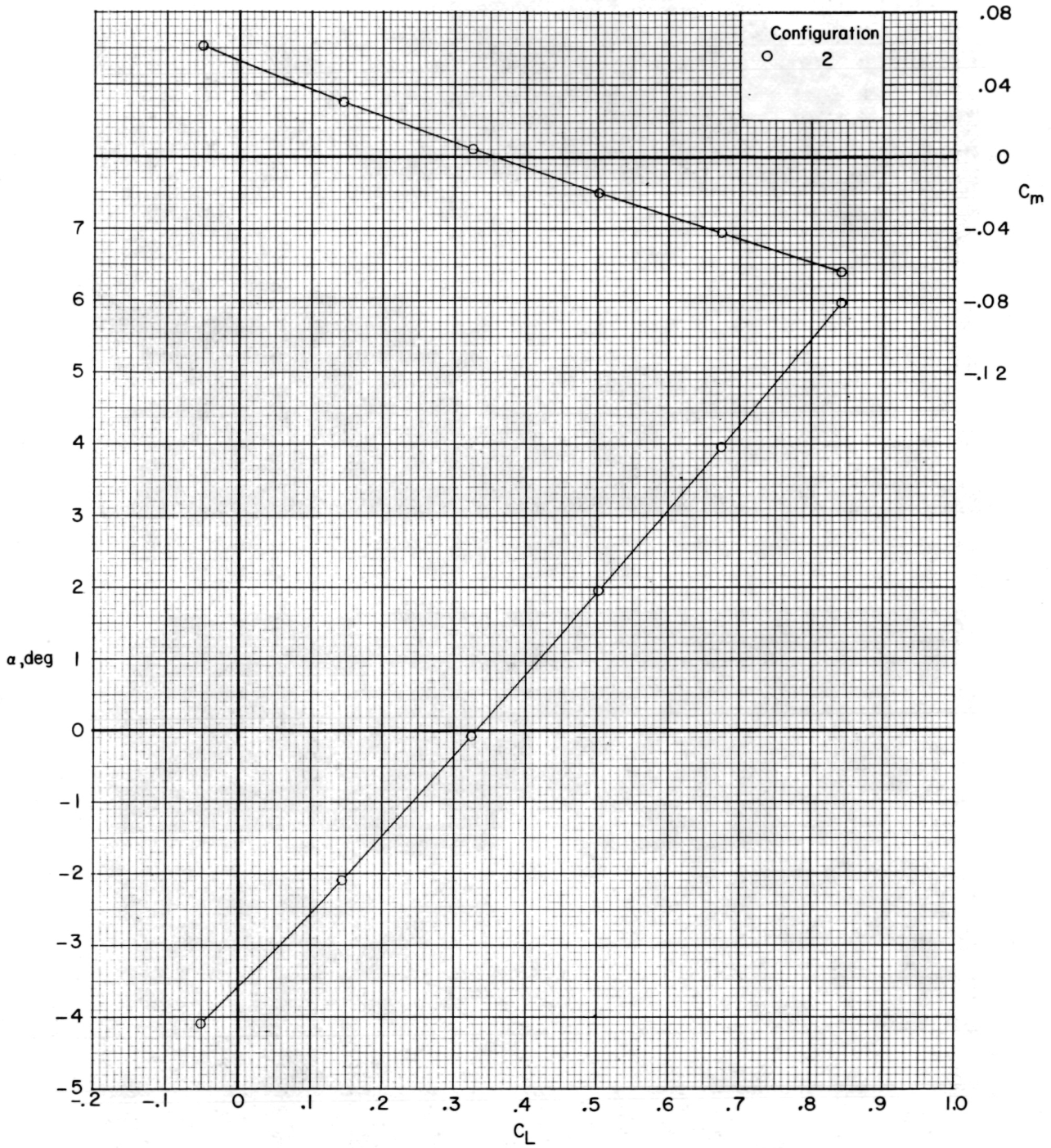

(a) M = 0.30; R = 2.00×10^6.

Figure 3.- Effect of airfoil contour on longitudinal aerodynamic characteristics.

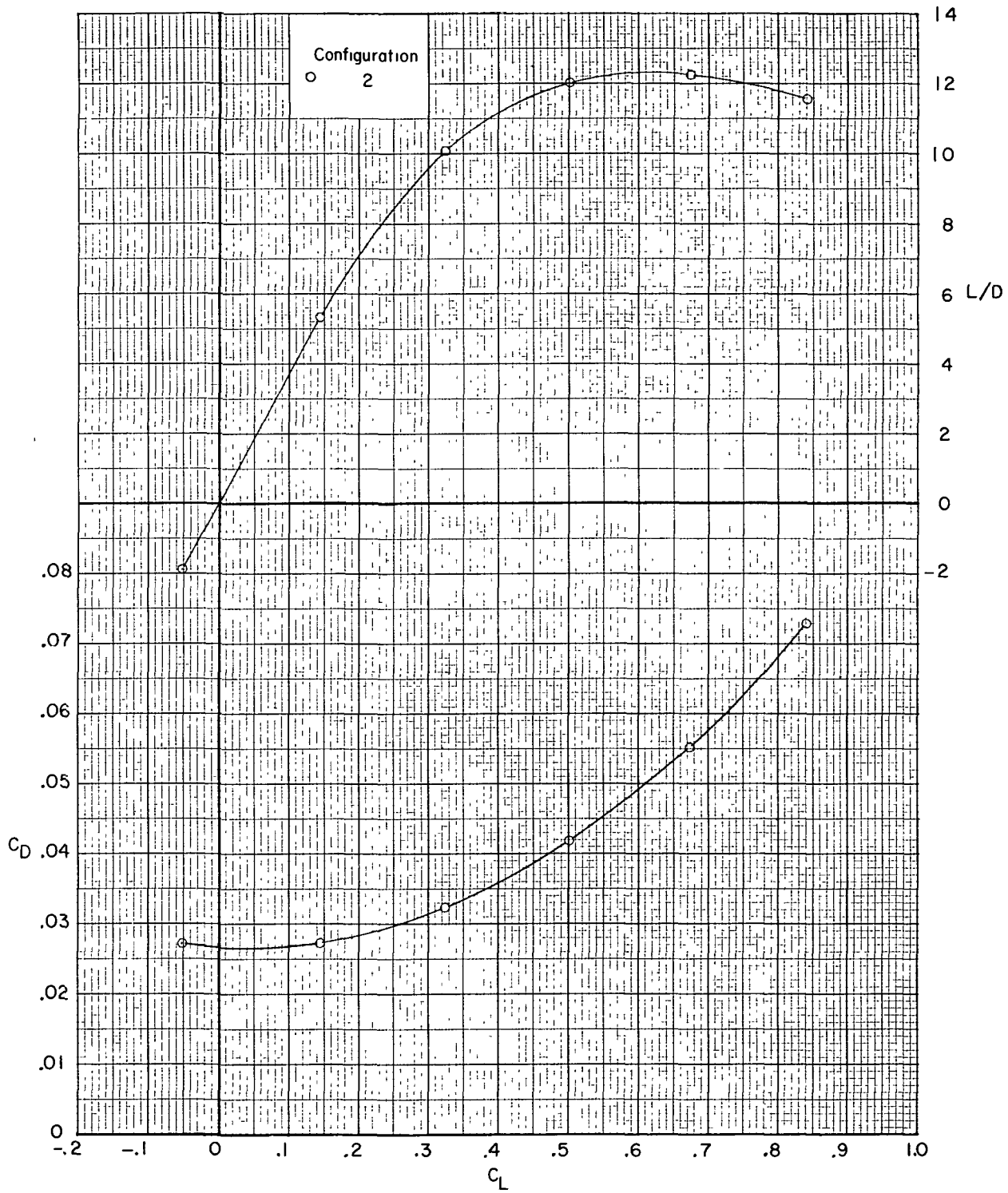

(a) Concluded.

Figure 3.- Continued.

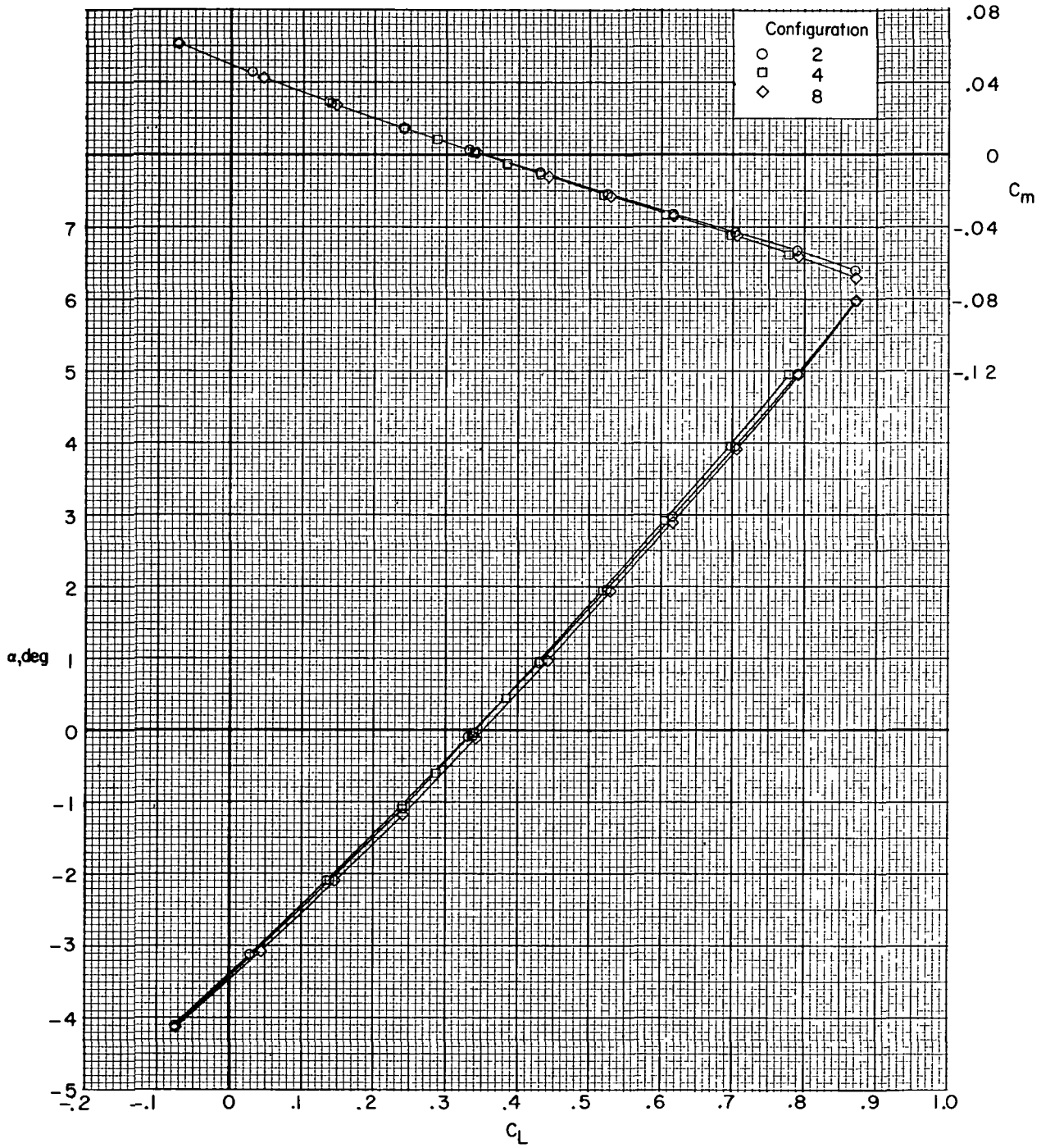

(b) M = 0.50; R = 2.66×10^6.

Figure 3.- Continued.

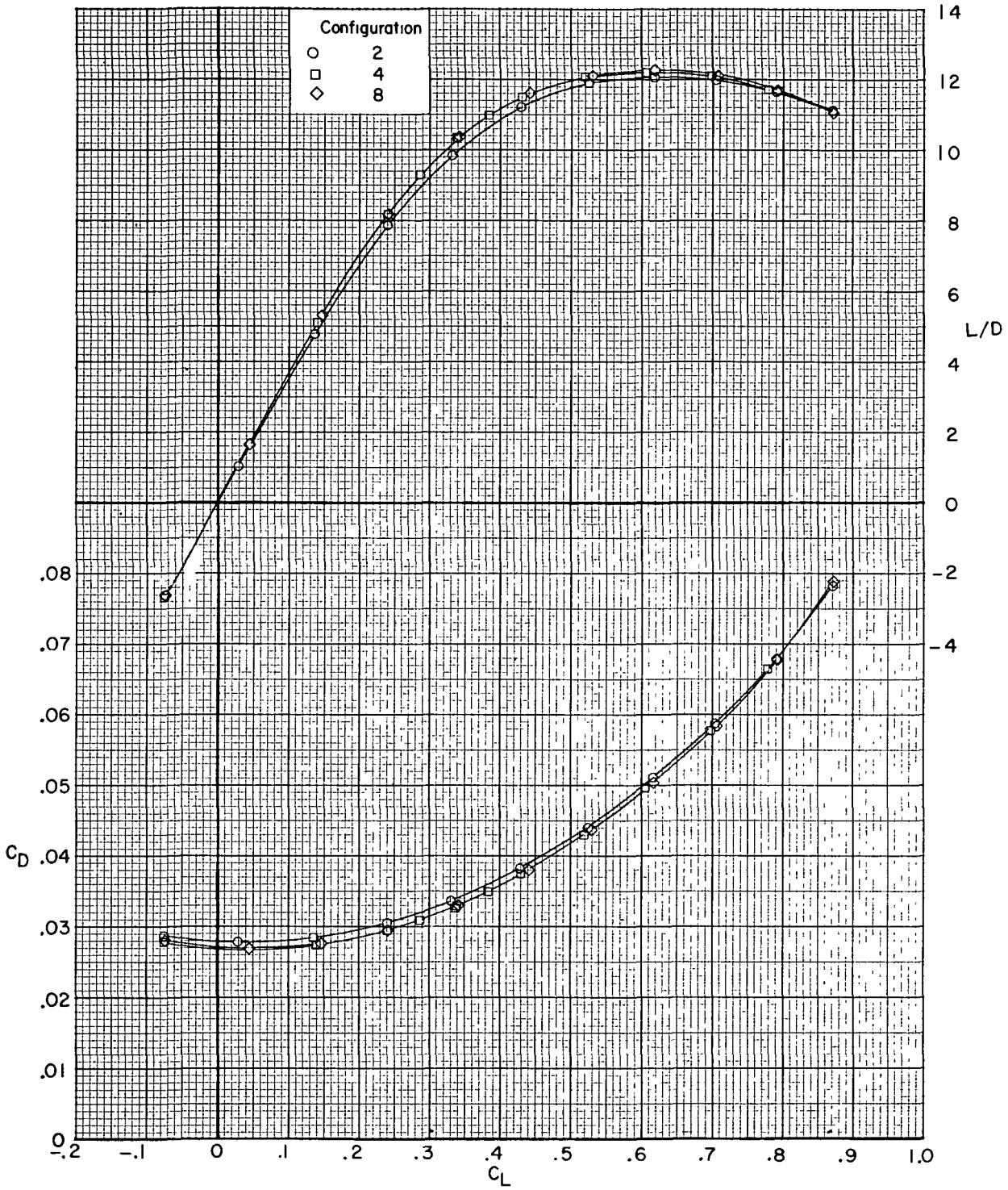

(b) Concluded.

Figure 3.- Continued.

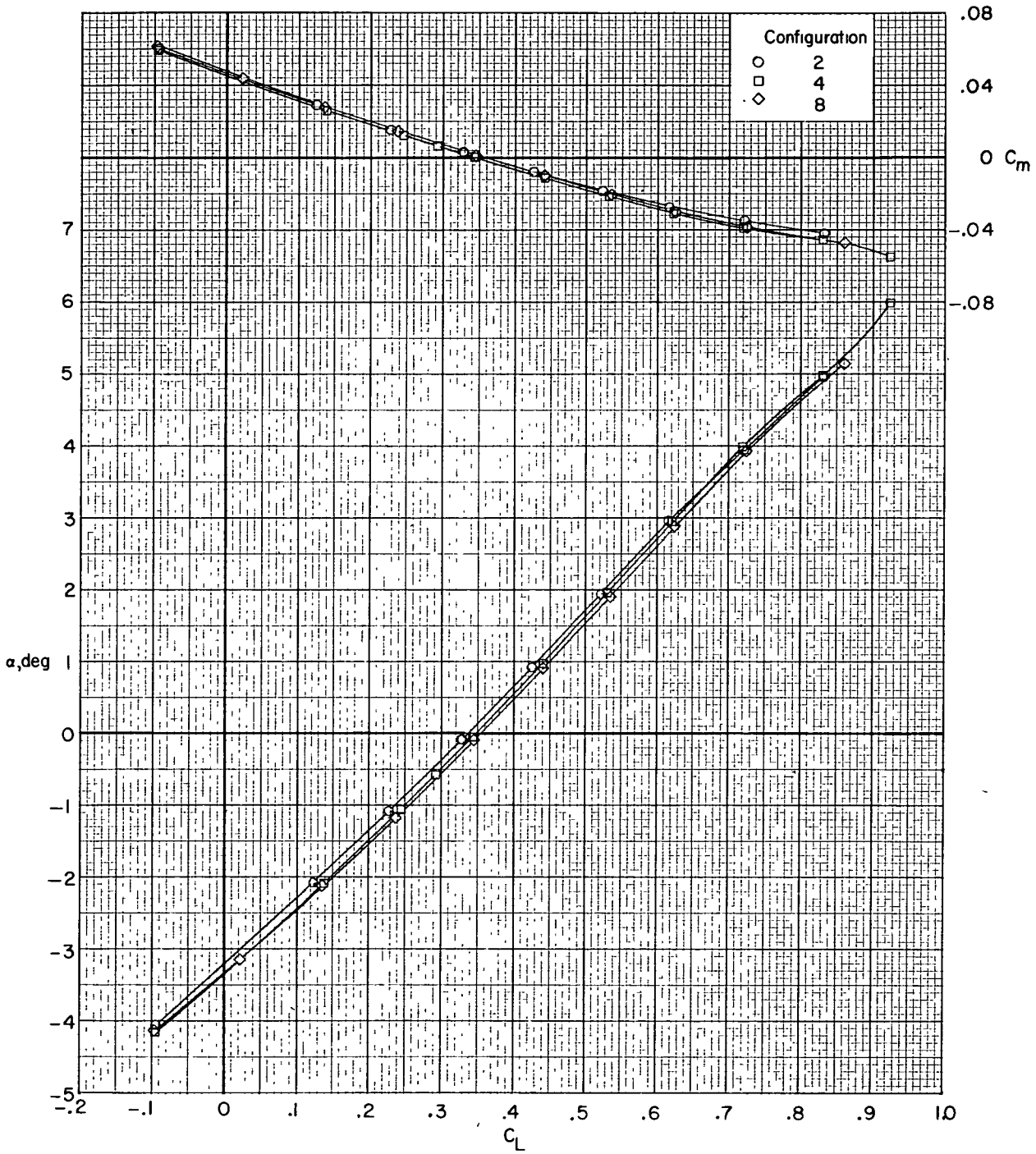

(c) M = 0.60; R = 3.33×10^6.

Figure 3.- Continued.

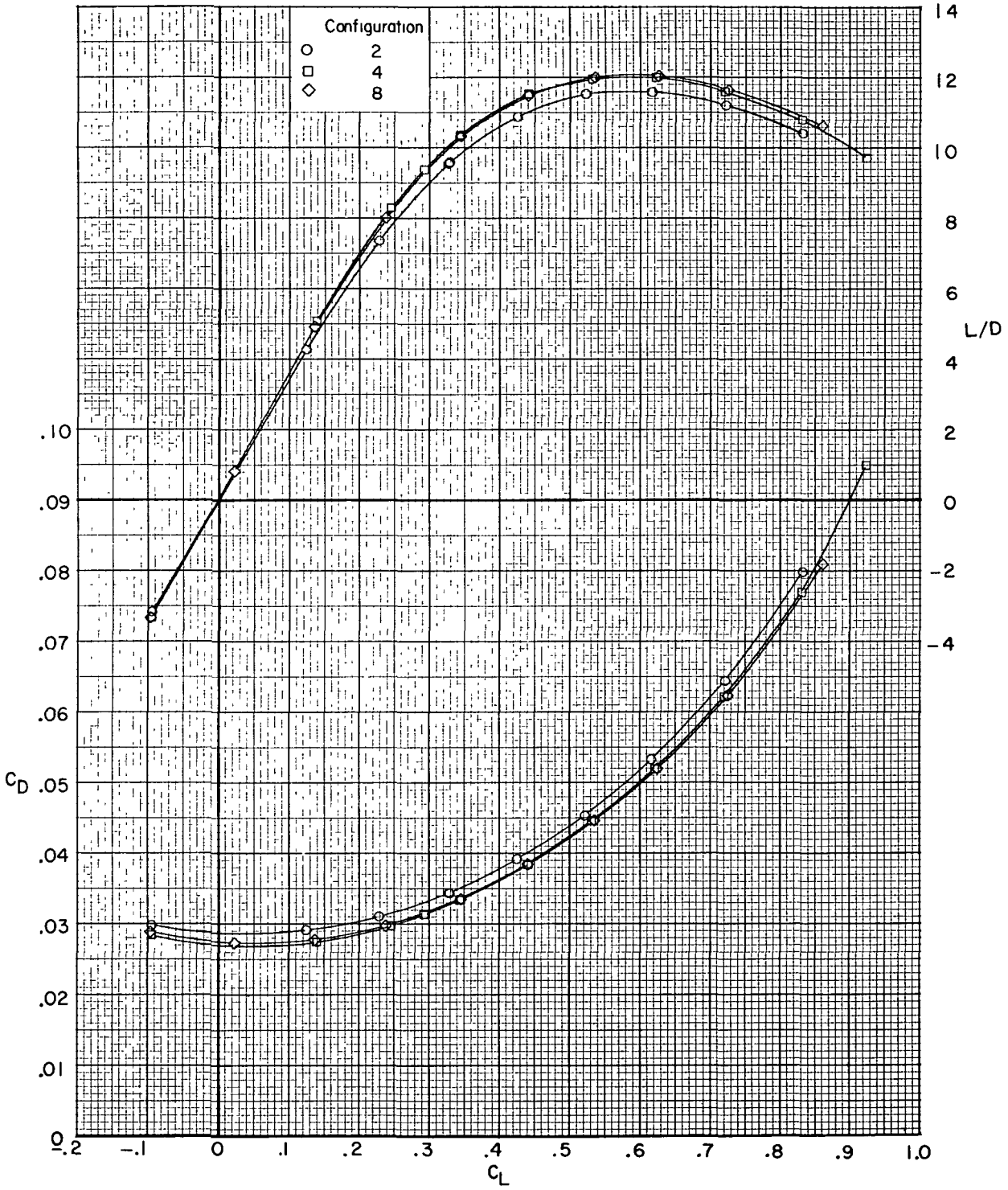

(c) Concluded.

Figure 3.- Continued.

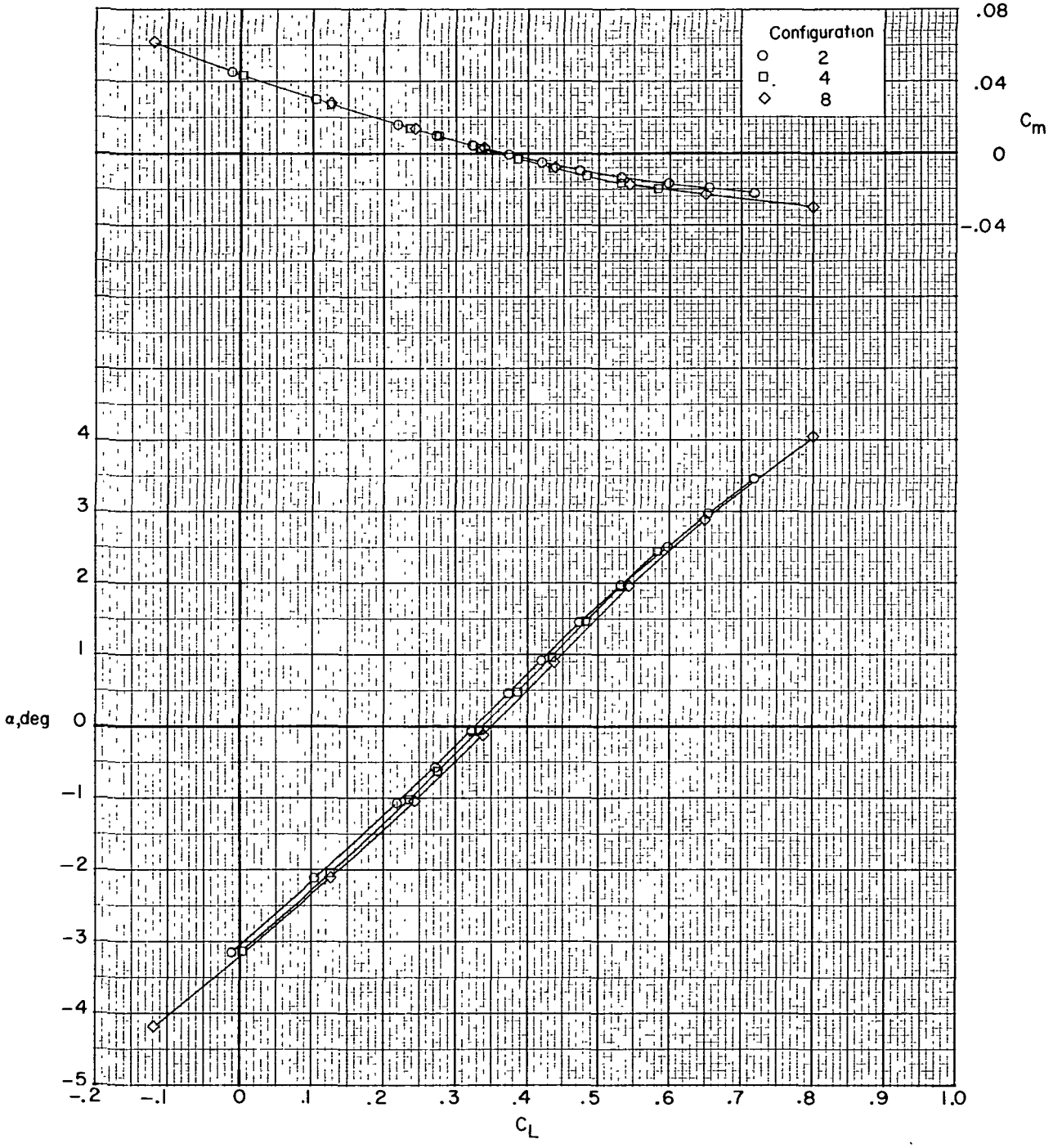

(d) M = 0.65; R = 3.86×10^6.

Figure 3.- Continued.

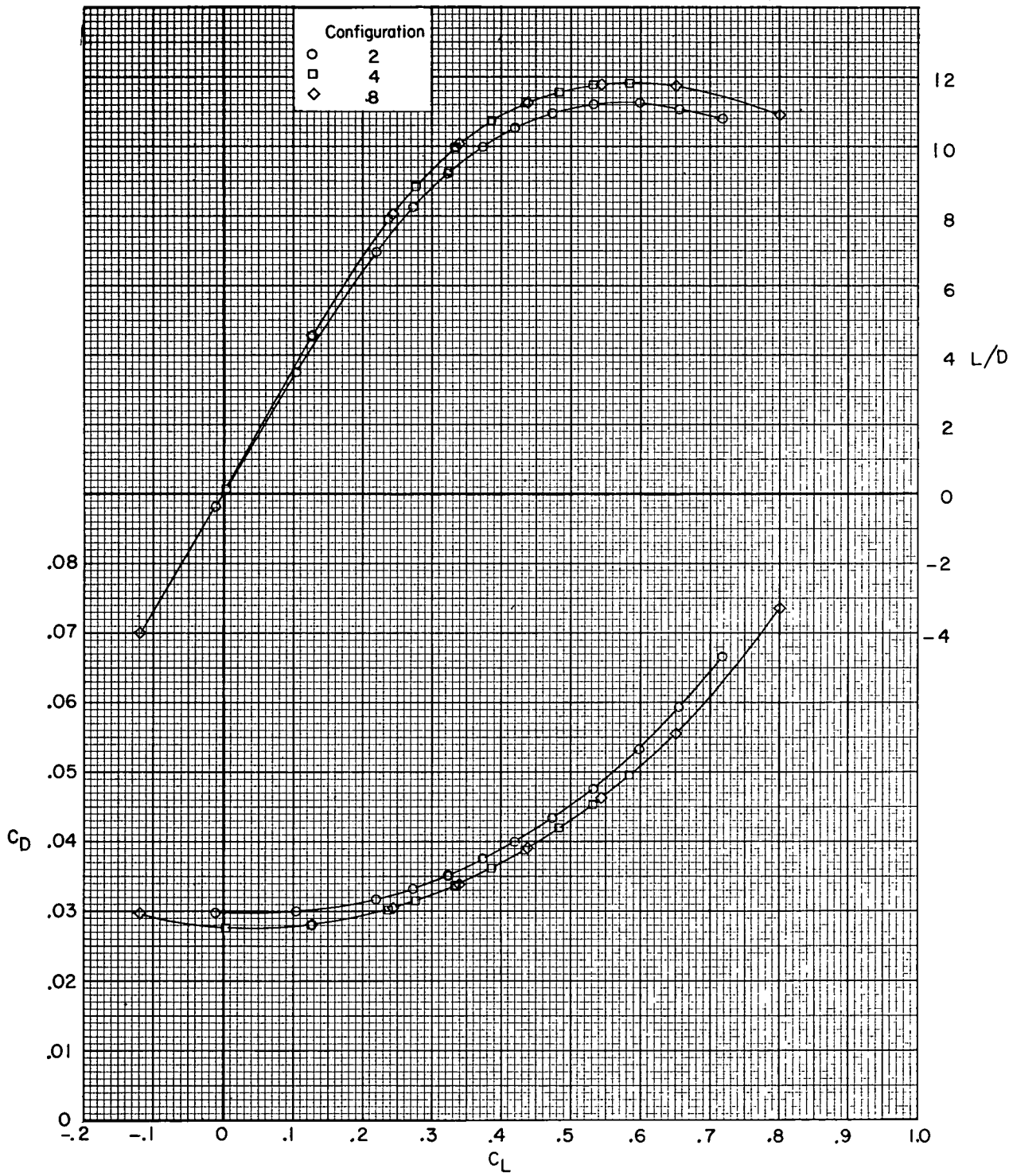

(d) Concluded.

Figure 3.- Continued.

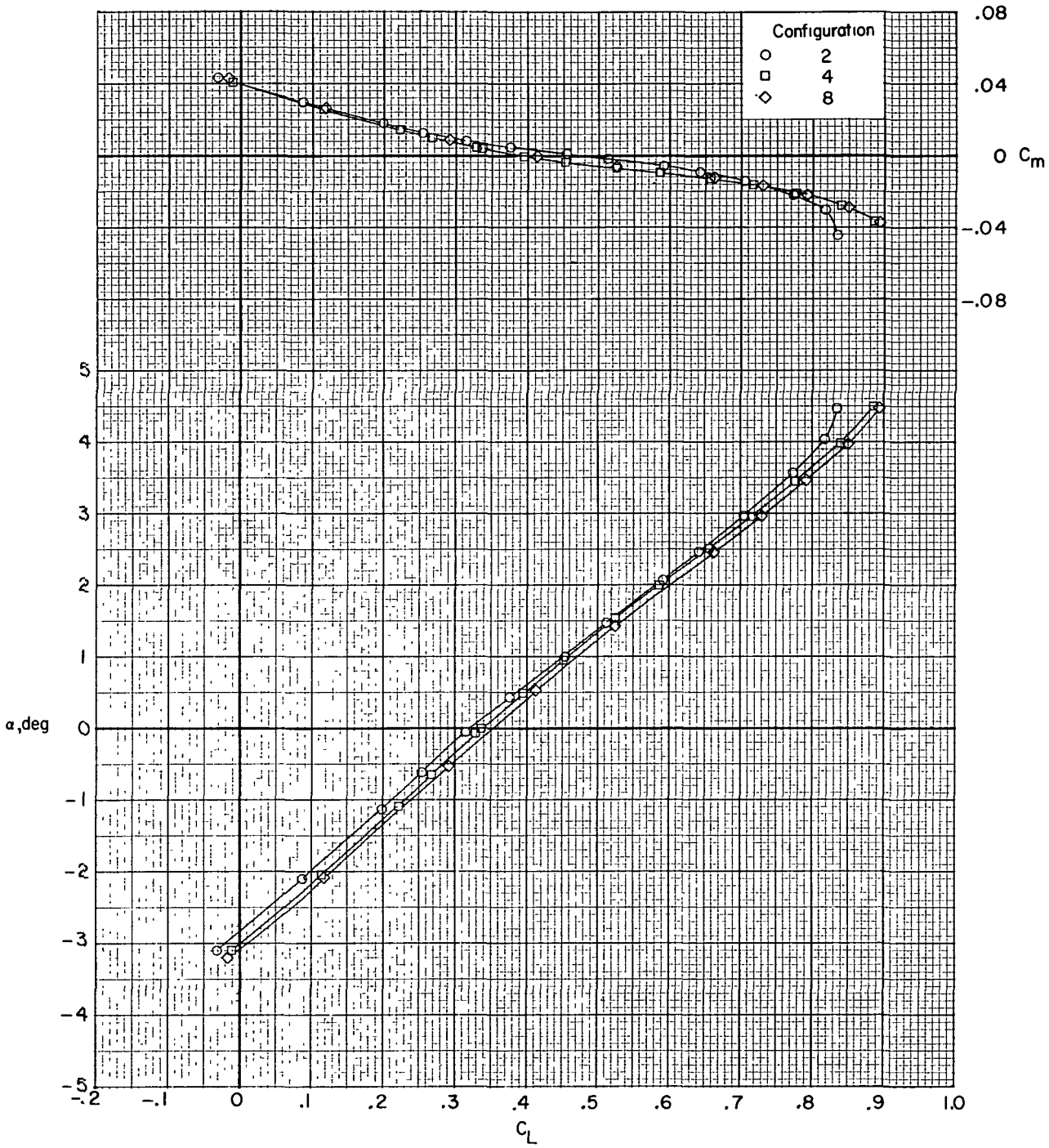

(e) M = 0.70; R = 3.86×10^6.

Figure 3.- Continued.

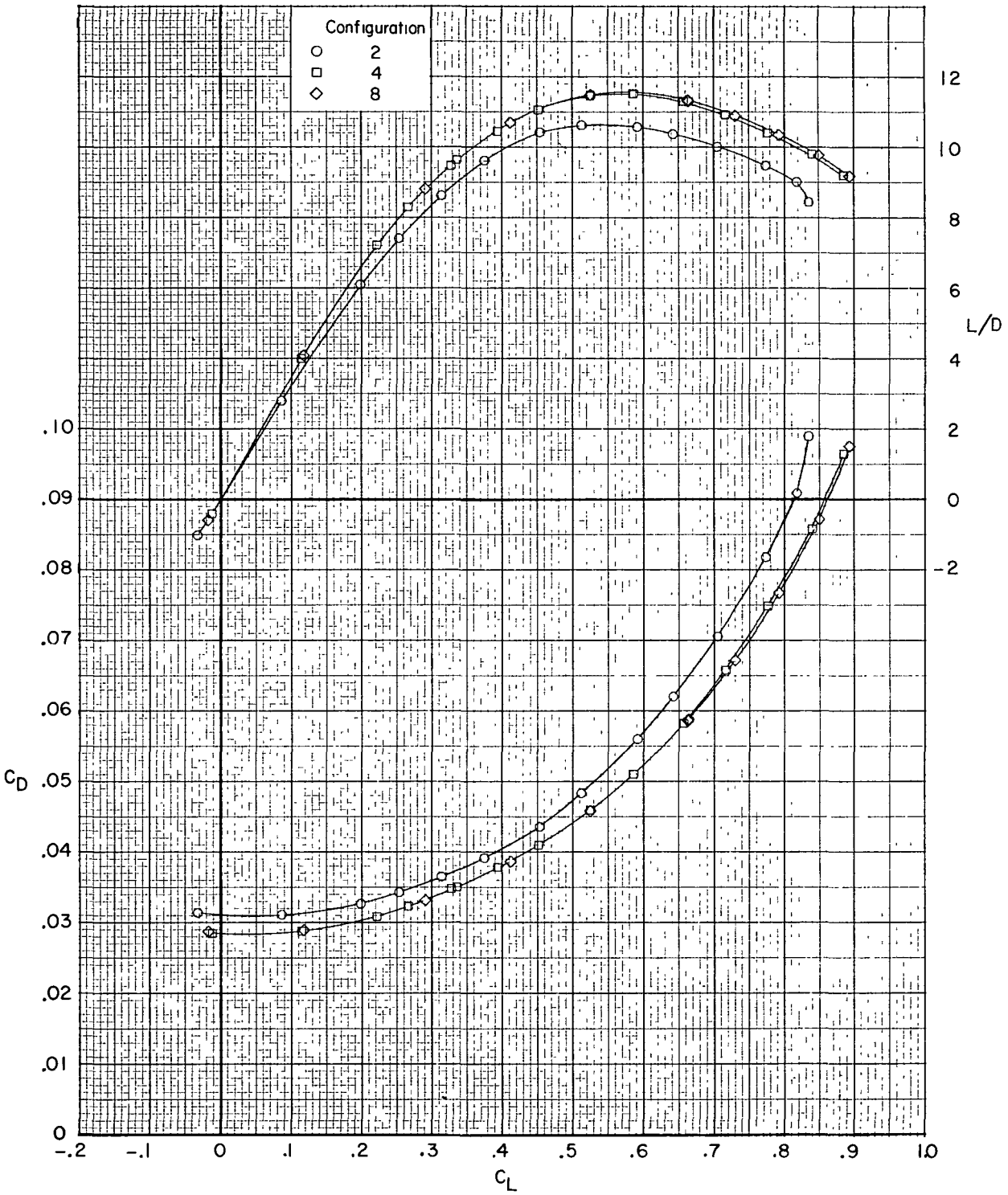

(e) Concluded.

Figure 3.- Continued.

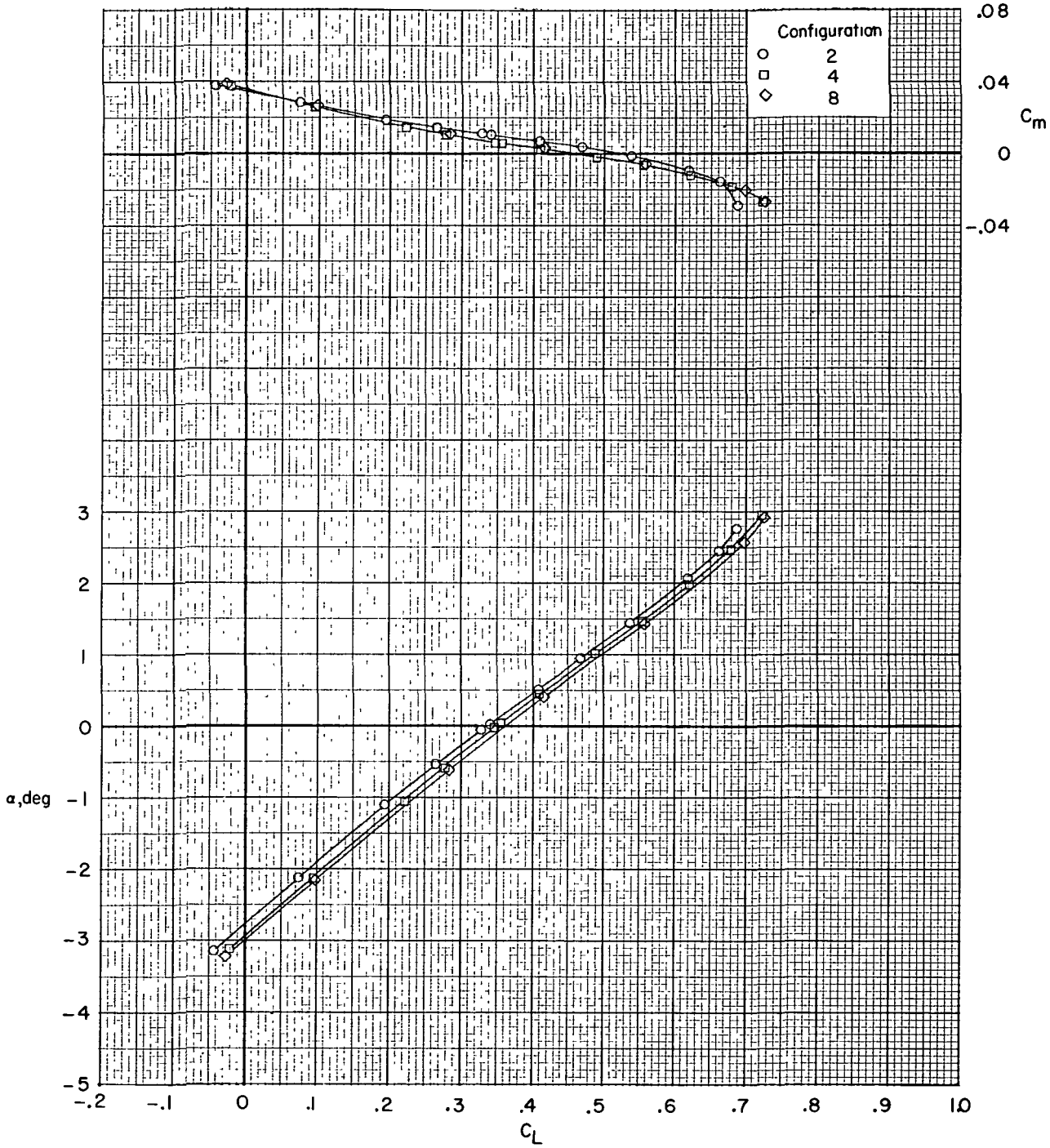

(f) M = 0.73; R = 3.86×10^6.

Figure 3.- Continued.

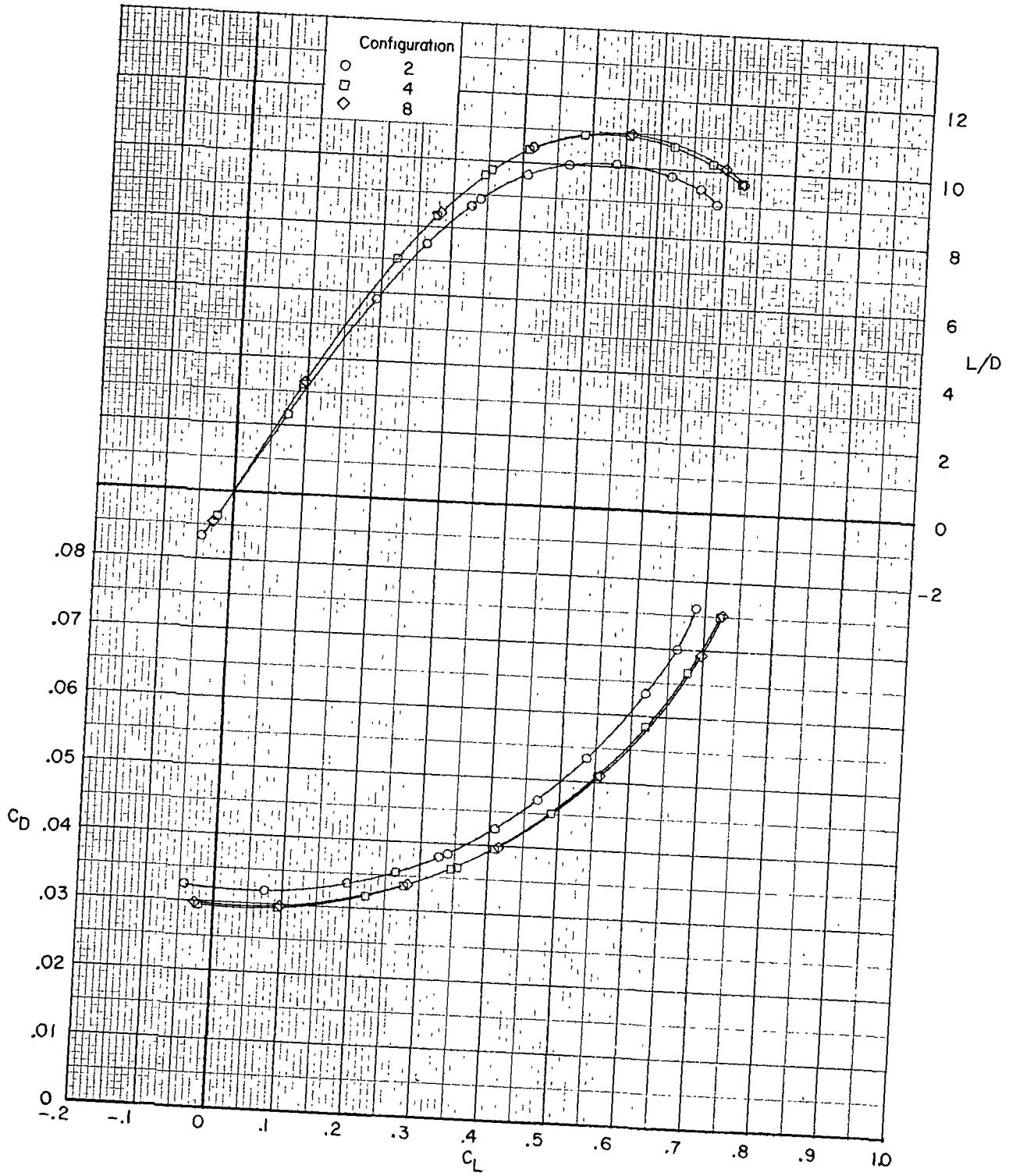

(f) Concluded.

Figure 3.- Continued.

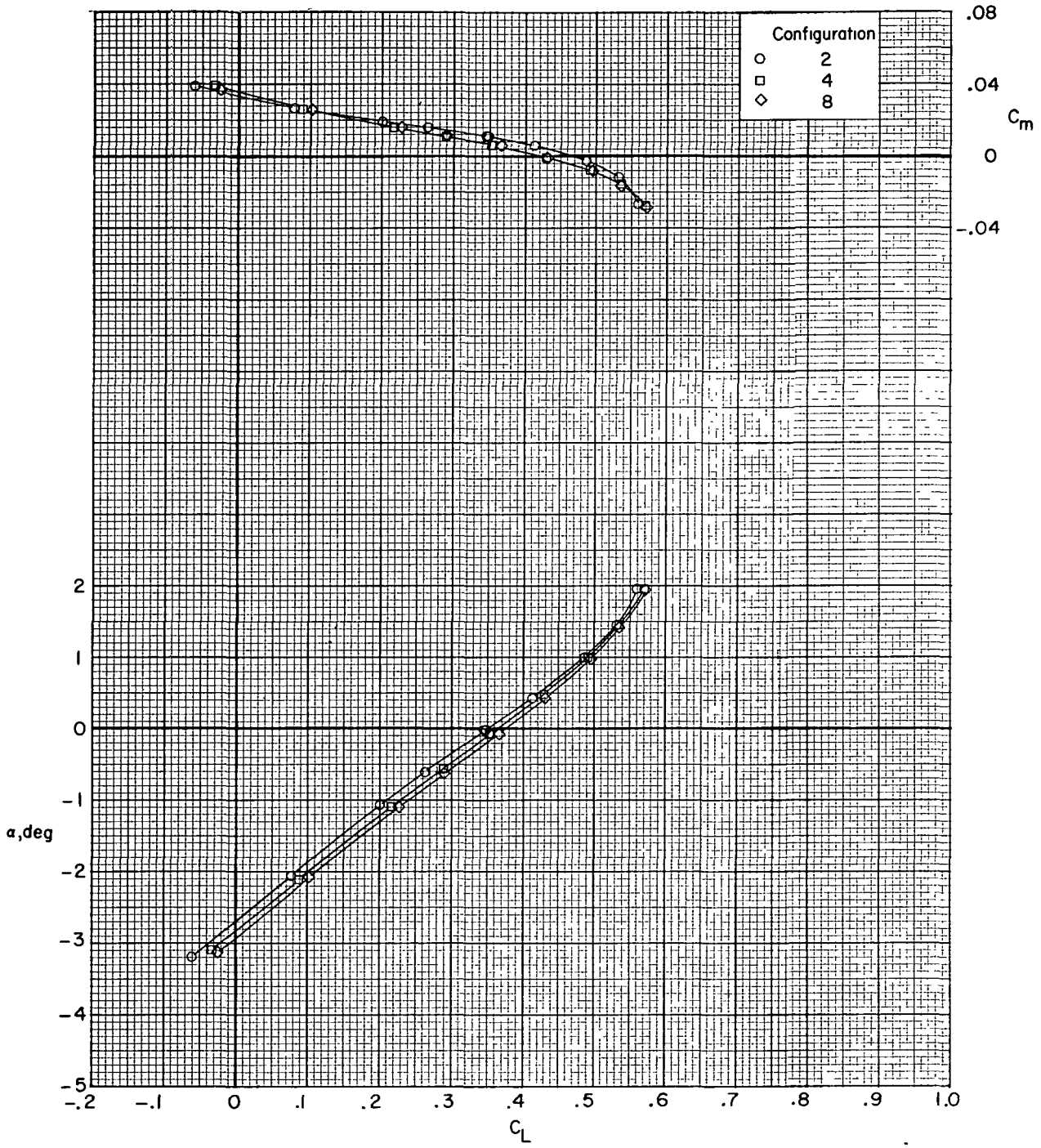

(g) M = 0.75; R = 3.86×10^6.

Figure 3.- Continued.

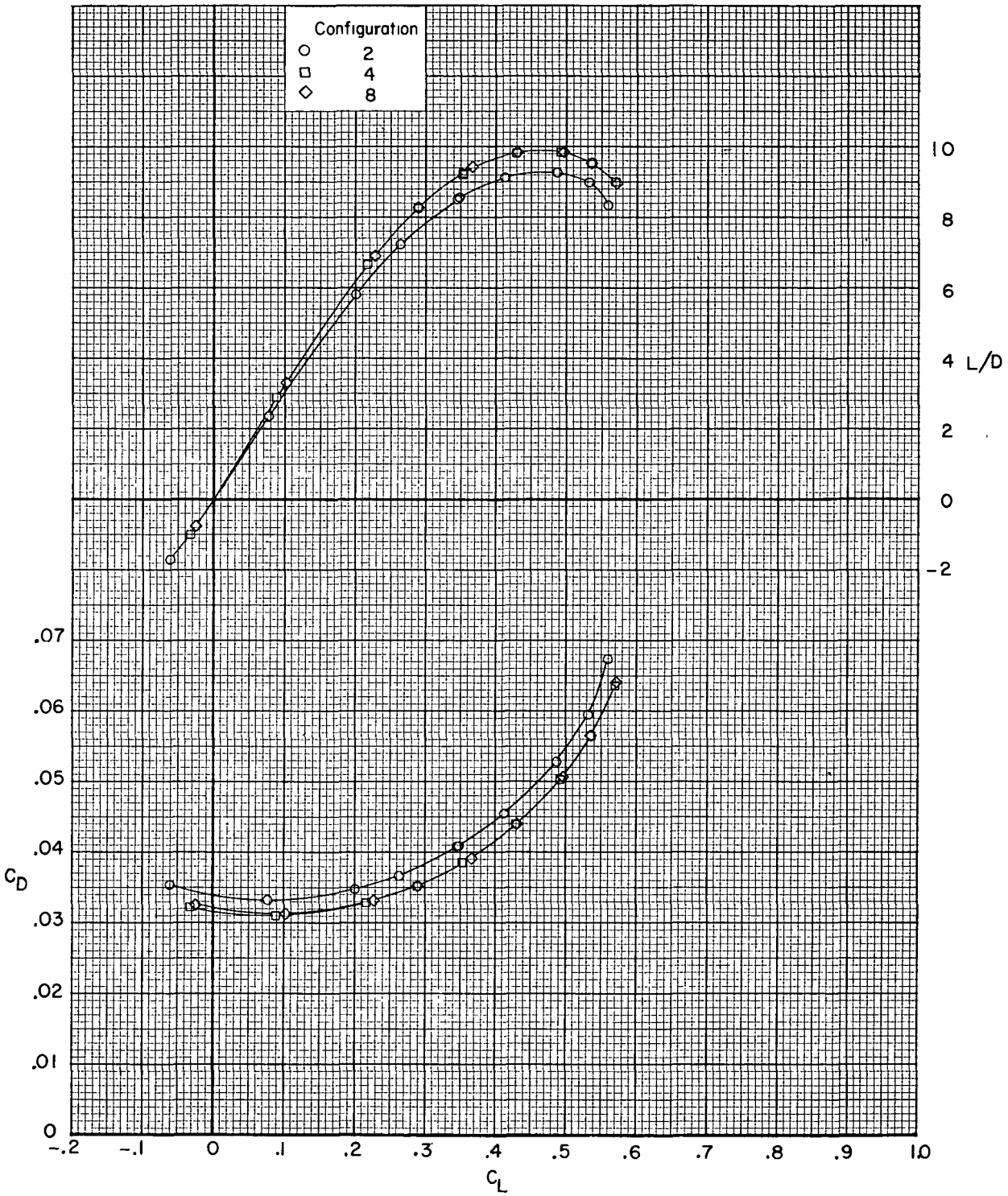

(g) Concluded.

Figure 3.- Continued.

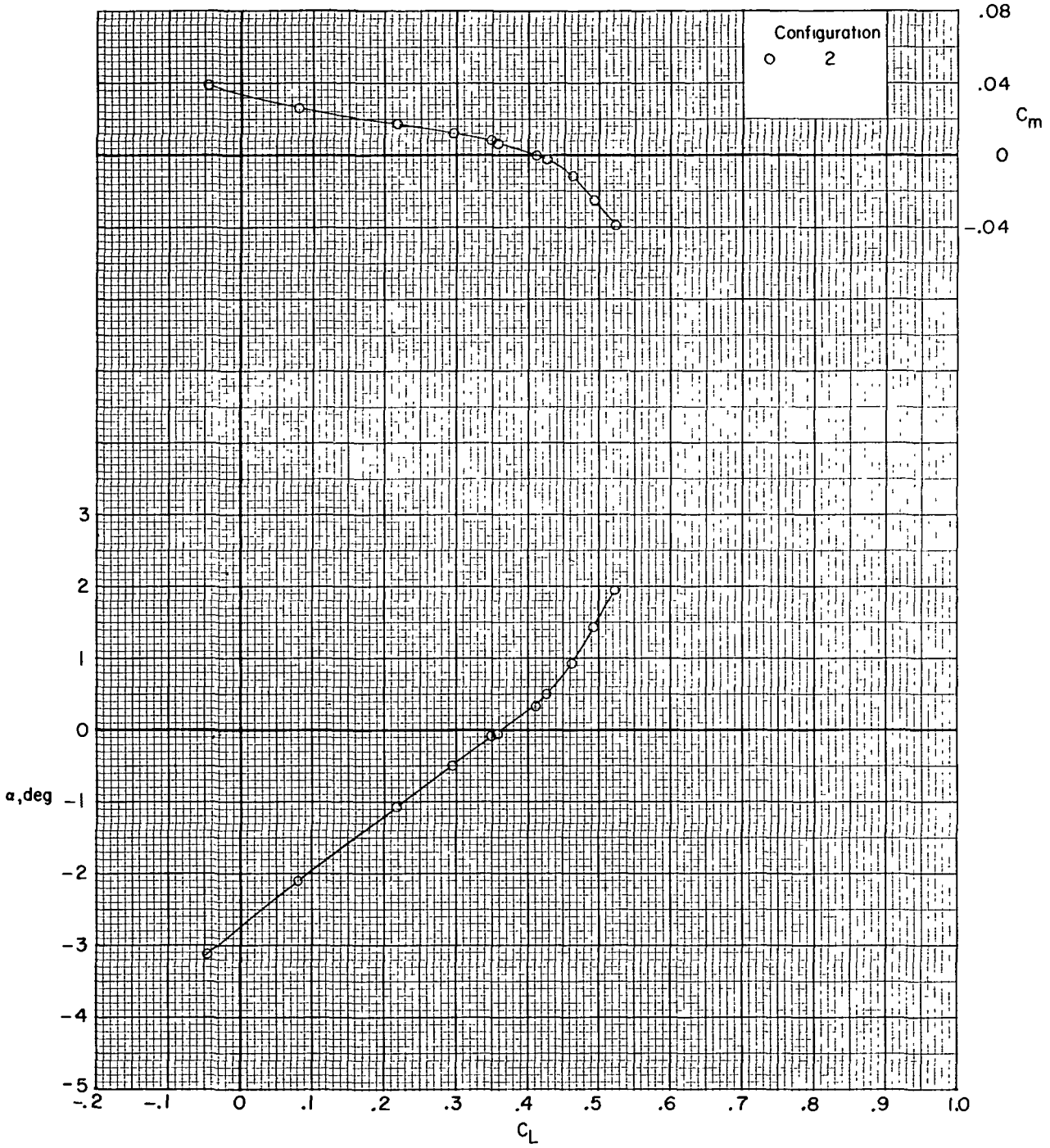

(h) M = 0.76; R = 3.86×10^6.

Figure 3.- Continued.

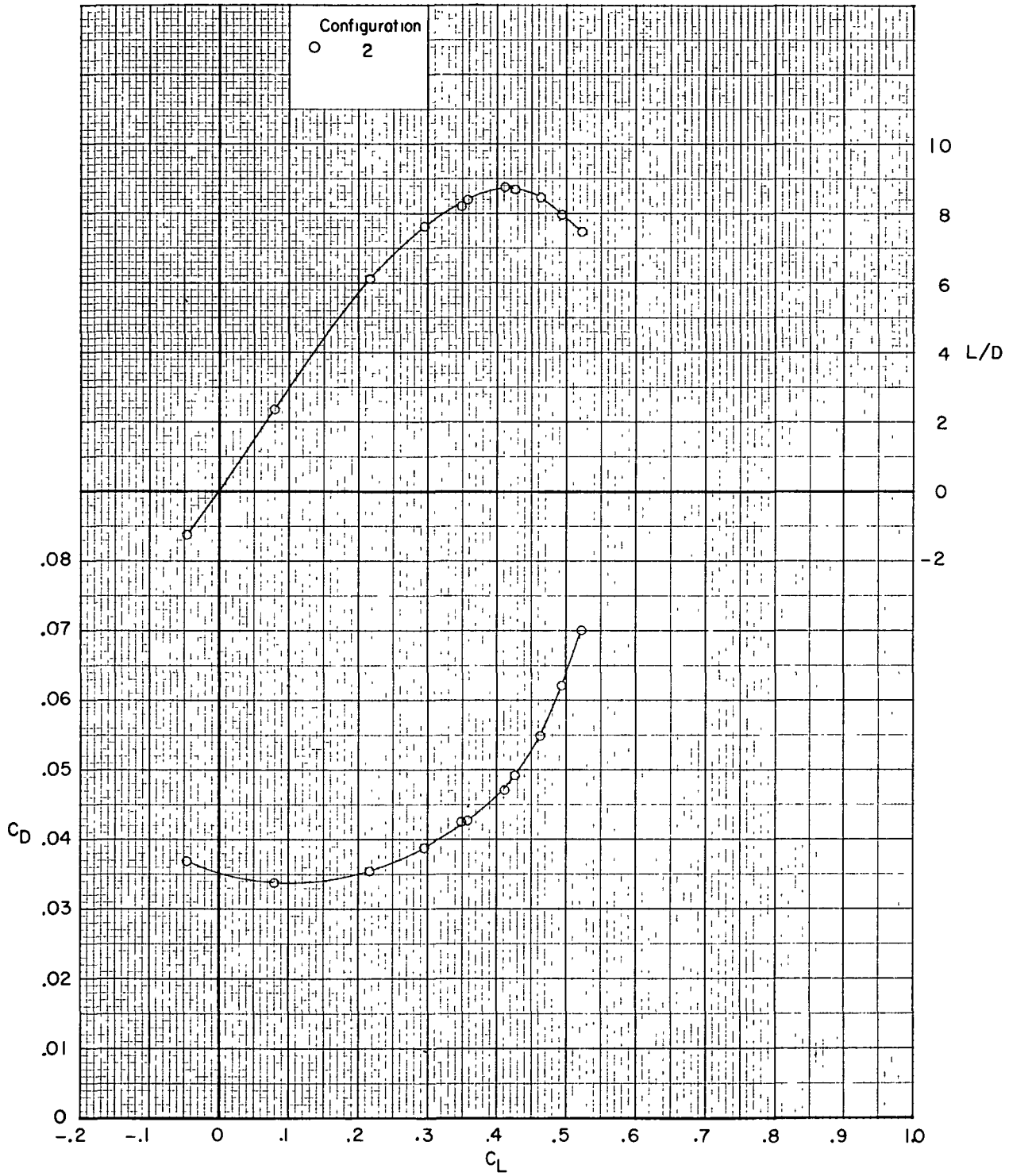

(h) Concluded.

Figure 3.- Concluded.

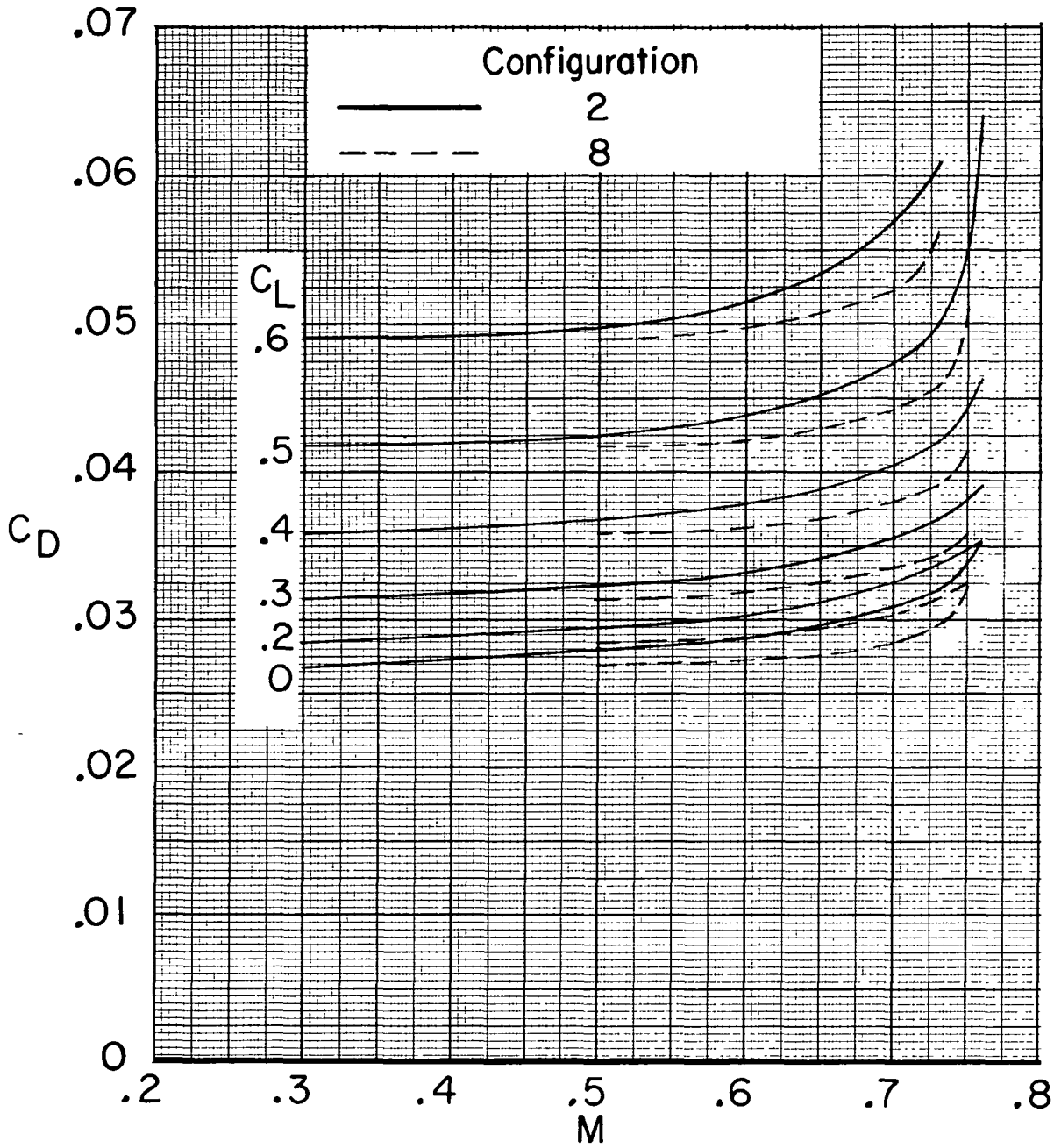

Figure 4.- Variation of drag coefficient with Mach number.

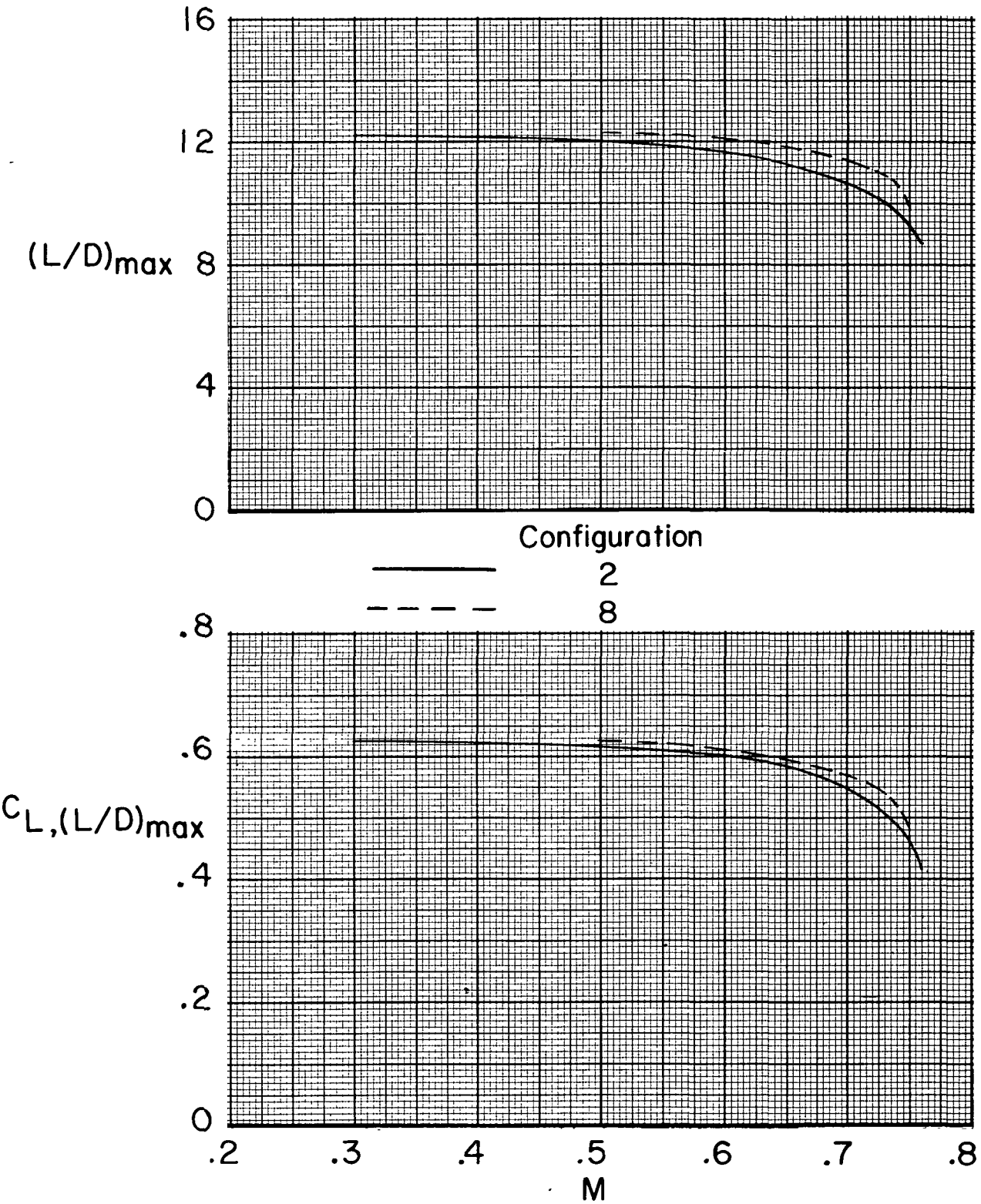

Figure 5.- Variation of untrimmed maximum lift-drag ratio and lift coefficient at $(L/D)_{max}$ with Mach number.

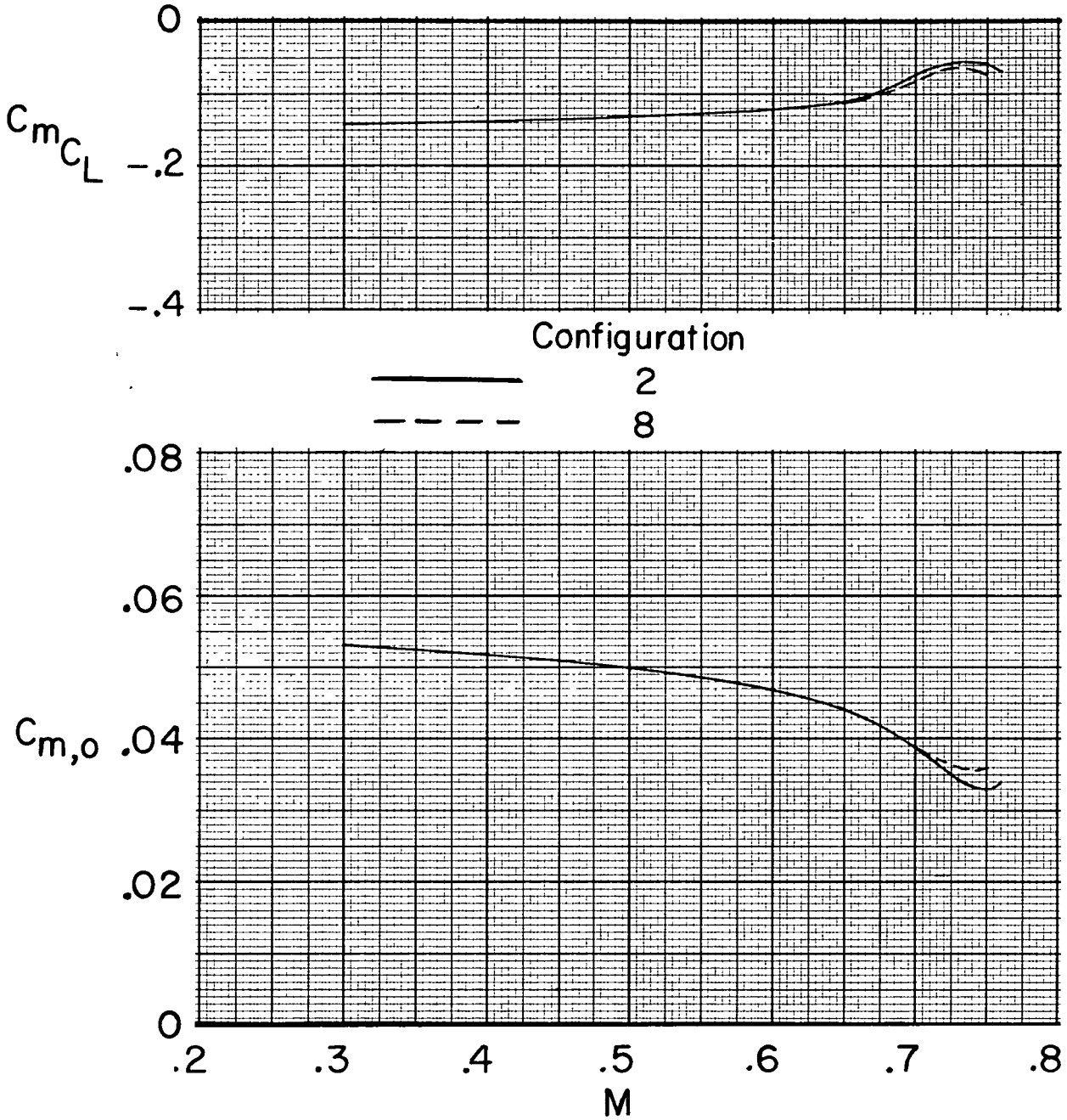

Figure 6.- Variation of the longitudinal stability derivative and zero-lift pitching moment with Mach number. $C_L = 0.3$.

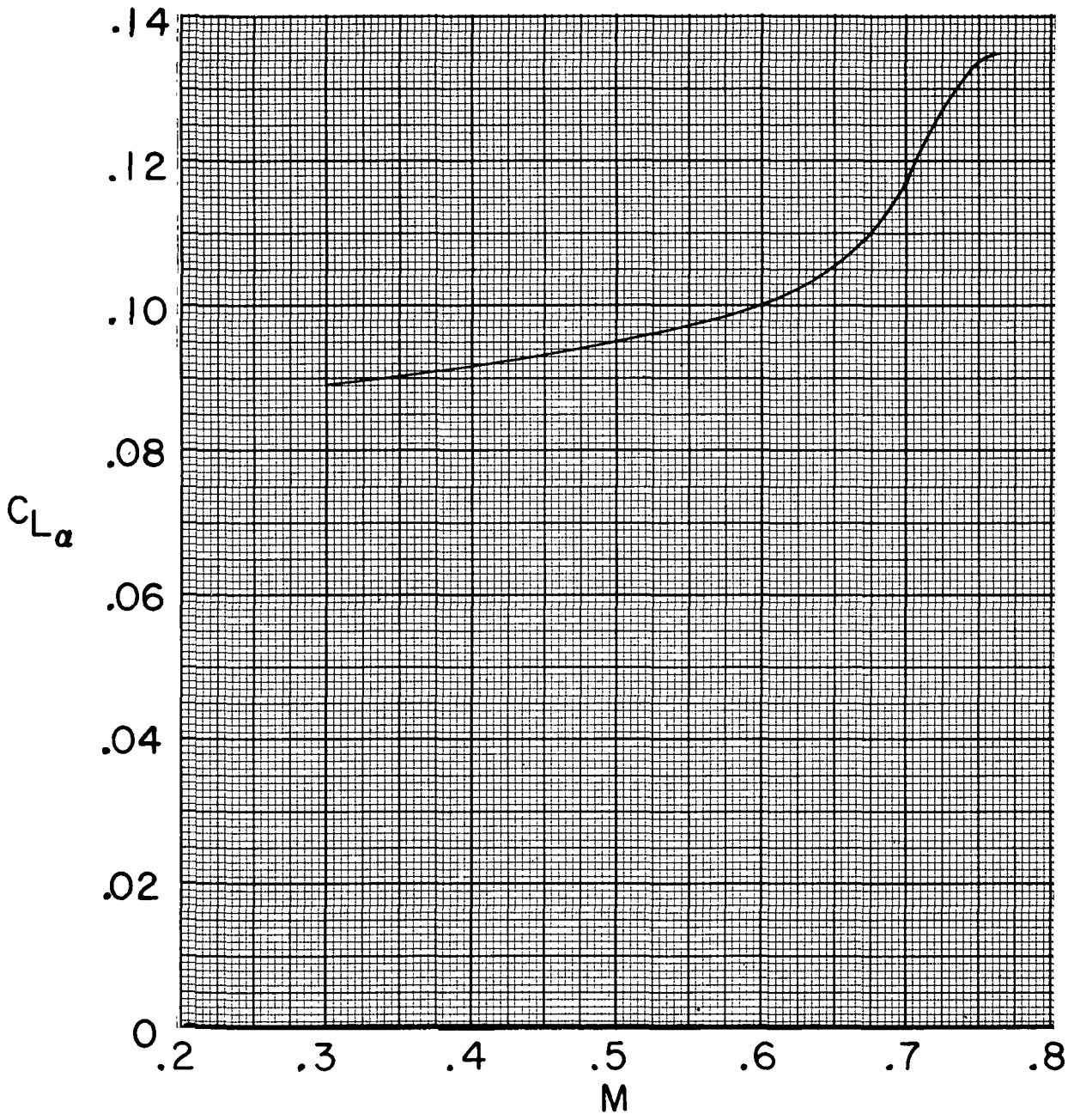

Figure 7.- Variation of lift-curve slope with Mach number.
Configuration 2; $C_L = 0.3$.

[redacted]

"The aeronautical and space activities of the United States shall be conducted so as to contribute . . . to the expansion of human knowledge of phenomena in the atmosphere and space. The Administration shall provide for the widest practicable and appropriate dissemination of information concerning its activities and the results thereof."

— NATIONAL AERONAUTICS AND SPACE ACT OF 1958

NASA SCIENTIFIC AND TECHNICAL PUBLICATIONS

TECHNICAL REPORTS: Scientific and technical information considered important, complete, and a lasting contribution to existing knowledge.

TECHNICAL NOTES: Information less broad in scope but nevertheless of importance as a contribution to existing knowledge.

TECHNICAL MEMORANDUMS: Information receiving limited distribution because of preliminary data, security classification, or other reasons.

CONTRACTOR REPORTS: Scientific and technical information generated under a NASA contract or grant and considered an important contribution to existing knowledge.

TECHNICAL TRANSLATIONS: Information published in a foreign language considered to merit NASA distribution in English.

SPECIAL PUBLICATIONS: Information derived from or of value to NASA activities. Publications include conference proceedings, monographs, data compilations, handbooks, sourcebooks, and special bibliographies.

TECHNOLOGY UTILIZATION PUBLICATIONS: Information on technology used by NASA that may be of particular interest in commercial and other non-aerospace applications. Publications include Tech Briefs, Technology Utilization Reports and Notes, and Technology Surveys.

Details on the availability of these publications may be obtained from:

SCIENTIFIC AND TECHNICAL INFORMATION OFFICE

NATIONAL AERONAUTICS AND SPACE ADMINISTRATION

Washington, D.C. 20546

[redacted]